



저작자표시-비영리-변경금지 2.0 대한민국

이용자는 아래의 조건을 따르는 경우에 한하여 자유롭게

- 이 저작물을 복제, 배포, 전송, 전시, 공연 및 방송할 수 있습니다.

다음과 같은 조건을 따라야 합니다:



저작자표시. 귀하는 원저작자를 표시하여야 합니다.



비영리. 귀하는 이 저작물을 영리 목적으로 이용할 수 없습니다.



변경금지. 귀하는 이 저작물을 개작, 변형 또는 가공할 수 없습니다.

- 귀하는, 이 저작물의 재이용이나 배포의 경우, 이 저작물에 적용된 이용허락조건을 명확하게 나타내어야 합니다.
- 저작권자로부터 별도의 허가를 받으면 이러한 조건들은 적용되지 않습니다.

저작권법에 따른 이용자의 권리는 위의 내용에 의하여 영향을 받지 않습니다.

이것은 [이용허락규약\(Legal Code\)](#)을 이해하기 쉽게 요약한 것입니다.

[Disclaimer](#)

A THESIS
FOR THE DEGREE OF MASTER OF ENGINEERING

Growth of Superconducting
 $\text{Bi}_2\text{Sr}_2\text{CaCu}_2\text{O}_{8+\delta}$ (Bi-2212) Single Crystal Whiskers
and the Characteristics

Sang-Yul Oh

Department of Mechatronics Engineering

GRADUATE SCHOOL

JEJU NATIONAL UNIVERSITY

2011. 08

**Growth of Superconducting
 $\text{Bi}_2\text{Sr}_2\text{CaCu}_2\text{O}_{8+\delta}$ (Bi-2212) Single Crystal Whiskers
and the Characteristics**

Sang-Yul Oh

(Supervised by Professor Sang-Jae Kim)

A thesis submitted in partial fulfillment of the requirement for the degree of Master of
Engineering

2011. 08

The thesis has been examined and approved.

Thesis director, Prof. Kyung-Ho Cho,	Department of Mechatronics Engineering, Jeju National University
---	---

Thesis committee Member, Prof. Gui-Shik Kim,	Department of Mechanical Engineering, Jeju National University
---	---

Thesis committee Member, Prof. Sang-Jae Kim,	Department of Mechatronics Engineering Jeju National University
---	--

August, 2011.

Department of Mechatronics Engineering
GRADUATE SCHOOL
JEJU NATIONAL UNIVERSITY
REPUBLIC OF KOREA

JEJU NATIONAL UNIVERSITY 1952



*dedicated to
my beloved wife,
my kids Seung-hyeok, Min-hyeok and Yu-ra*

ACKNOWLEDGEMENTS

Before starting the first thesis of my life it becomes my pious duty to say thanks to my guide Prof. Sang-Jae Kim, who introduced me to such an exciting and challenging field of Superconductivity. I am really fascinated by his style of working and at the same time his moral support that always kept my moral high.

I would like to acknowledge to department Prof. Kyung-Ho Cho, Prof. Joung-Hwan Lim, Prof. Kyung-Hyun Choi and Prof. Chul-Uoong Kang for their help and support during the course work. I would like also to acknowledge to Prof. Gui-Shik Kim for advice and boosted. I thank to Dr. Takeshi Hatano from National Institute for Materials Science, Tsukuba, Japan for providing us XRD pattern.

I cannot forget my lab mate Chang-Jo Heo, Gi-Young Kang, Yoo-Gyeom Kim, Si-O Kim, Suk-Koo Kim, Gwang-Yul Ko, Se-Na Ko, Gunashekar and Shrikant Saini they always encouraged me to perform better.

I am also grateful for the Research Instrument Center (RIC) at Jeju National University for providing me opportunities to handle many instrument facilities during my study.

This acknowledgement cannot be complete without mentioning the gratitude to my honorable parents, my wife and my kids (Seung-Hyeok, Min-Hyeok and Yu-Ra) for their belief in me and I'm unable to find proper words to express my feelings.

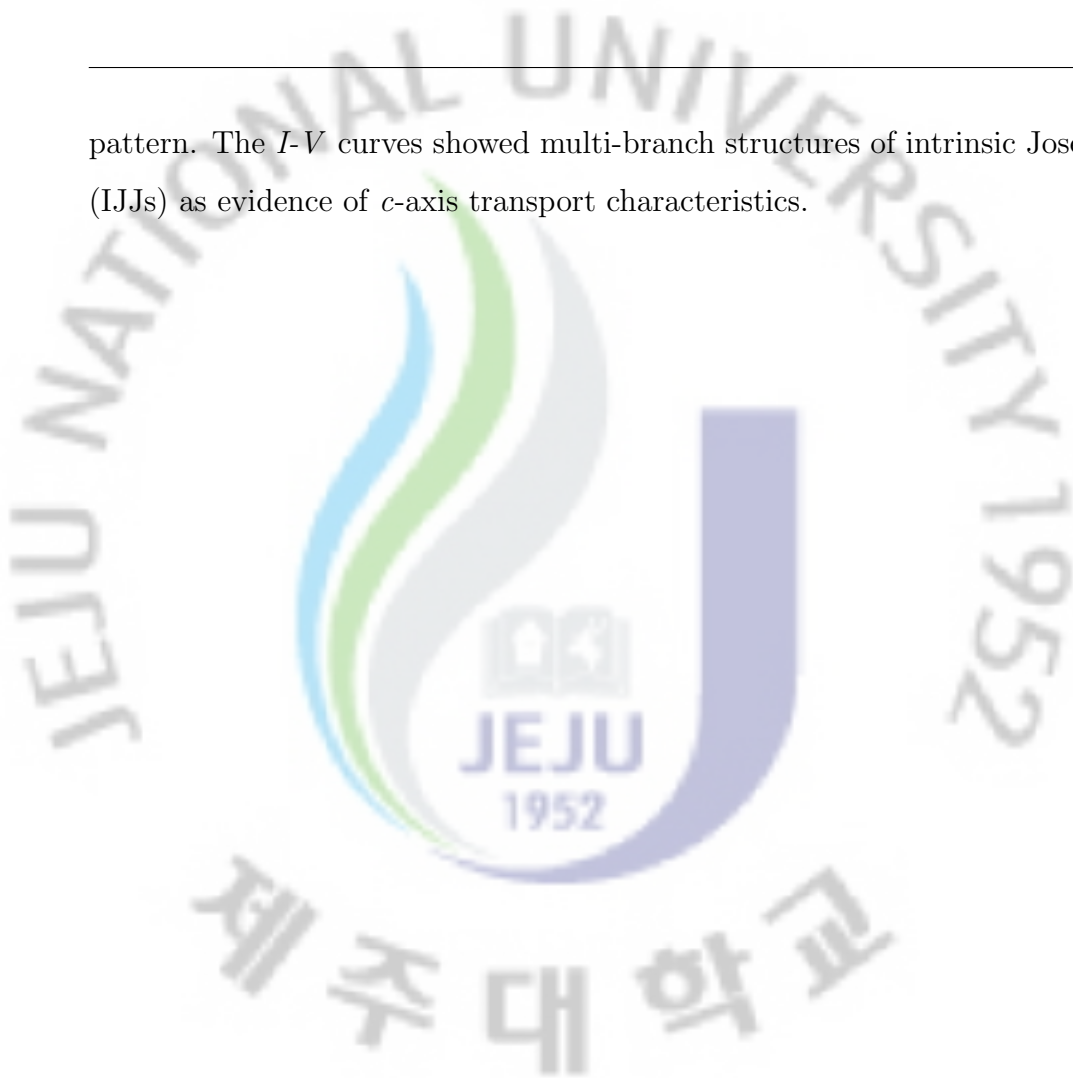
ABSTRACT

The single-crystal whiskers of $\text{Bi}_2\text{Sr}_2\text{CaCu}_2\text{O}_{8+\delta}$ (Bi-2212) have attracted much attention because they have perfect crystallinity, are free of dislocations, show peculiar dimensions with extremely small cross-sections, and have excellent superconducting properties. The developments suggest that whiskers might be used in the fabrication of new electronic devices using intrinsic Josephson junctions and related phenomena, such as Josephson plasma oscillations. Stacked junctions have been fabricated by using Bi-2212 whiskers and are thought to be prospective candidates for high-frequency applications of the intrinsic Josephson effect.

All studies on Bi-2212 whisker growth so far have been based on flux flow method. The whiskers are grown by annealing only melt-quenched glassy precursors that dope Al. We have successfully grown Bi-2212 whiskers directly from the sintered pellets of polycrystalline precursor including Te that had not passed through a melt-quenched glassy state. These whiskers have excellent crystallinity with a small amount of Bi-2223 intergrowth and a very uniform multibranch structure of the current (I) - voltage (V) characteristics due to the intrinsic Josephson junctions along the *c*-axis, suggesting that the whiskers are homogeneous and of good quality.

We have succeeded in the growth of superconducting Bi-2212 single crystal whiskers with a Te-doped method. We use a Te-doped precursor with the mixed pure powders Bi_2O_3 , SrCO_3 , CuO and TeO_2 into the ratios of $\text{Bi}_2\text{Sr}_2\text{Ca}_2\text{Cu}_{2.5}\text{Te}_{0.5}\text{O}_x$. Bi-2212 single crystal whiskers have grown through the pellet surface 2-4 mm in length and 20-100 μm in width. Characteristics of whiskers were investigated by the resistance-temperature (*R-T*), X-ray diffraction (XRD) and current-voltage (*I-V*) measurements. The *R-T* characteristics in *ab*-plane of the whiskers showed that their $T_{c,on}$ and $T_{c,end}$ were about 106 K and 75 K, respectively and confirmed that the whiskers had Bi-2212 single crystal phase by XRD

pattern. The I - V curves showed multi-branch structures of intrinsic Josephson junctions (IJJs) as evidence of c -axis transport characteristics.



CONTENTS

1. Introduction	2
1.1 Introduction	2
1.2 Josephson Junction	3
1.3 Intrinsic Josephson junctions	4
1.4 Applications	5
1.4.1 Single Electron Transistor (SET)	5
1.4.2 Terahertz Application	5
1.5 Summary	9
2. Growth of Bi-2212 single crystal whiskers	11
2.1 Introduction	11
2.2 The growth process	12
2.3 Results and discussion	12
2.4 Summary	19
3. Three-Dimensional Focused Ion Beam Milling Technique	20
3.1 Introduction	20
3.2 The Focused Ion Beam	20
3.2.1 Fundamental Operating Principle of FIB	22
3.3 Fabrication of Josephson junctions	22
3.4 Summary	24
4. Intrinsic Josephson junctions Stack of Bi-2212	25
4.1 Introduction	25
4.2 Experimental details	27

4.3 Results and discussion	32
4.4 Summary	33
5. Conclusions	34



LIST OF FIGURES

1.1	The schematic of a Josephson junctions.	3
1.2	Schematic of intrinsic Josephson junctions with axial representation.	6
1.3	Schematic of SET along with a fabricated device in Bi-2212 single crystal whisker taken from ref. 21.	8
1.4	Schematic of terahertz device using layered superconductor. (Figure by Prof. H.-J. Lee, POSTECH.)	10
2.1	The heat treatment process to grow Bi-2212 single crystal whiskers.	13
2.2	An optical microscope image of as grown single crystal whiskers on the precursor pellet.	14
2.3	A SEM image to see the smooth surface of Bi-2212 single crystal whisker.	15
2.4	Four probe configuration for electrical characterizations.	16
2.5	X-ray diffraction patterns of as-grown Bi-based whiskers prepared at 870 °C for 100 h in oxygen flow rates of 150 ml/min.	17
2.6	X-ray diffraction patterns of as-grown Bi-based whiskers prepared at 870 °C for 100 h in oxygen flow rates of 300 ml/min.	18
3.1	A picture of FIB machine (SII NanoTechnology SMI2050) in Research Institute of Center (RIC).	21
3.2	The steps of fabrication process of Josephson junctions by FIB. (a) The inclined sample stage where we mount a sample. (b) A side view of as mounted sample on sample stage. (c) The first etching process to mill junctions in-plane area. (d) The final etching in two grooves.	23
4.1	The red arrow indicates the direction of current to measure the characteristics of IJJs in Bi-2212 single crystal whiskers.	26

4.2	FIB image of stack and schematic of the IJJs configuration in the stack. The blue arrow indicates the direction of current flow which is along the IJJs.	28
4.3	The resistance vs. temperature characteristics of the stack in ab -plane. . .	29
4.4	The current (I) vs. voltage (V) characteristics of the stack at 10 K.	30
4.5	The current (I) vs. voltage (V) characteristics at low biasing of the stack at 10 K.	31



LIST OF TABLES

1.1	Various application of superconductivity	7
2.1	Typical conditions for whisker growth: the nominal compositions of precursors and oxygen flow rates	13

1. INTRODUCTION

1.1 Introduction

Superconductivity was discovered in 1911 by the Dutch physicist Heike Kamerlingh Onnes. He dedicated his entire career to exploring extremely cold refrigeration. In 1908, he successfully liquified helium by cooling it into 4 K. In 1911, he started investigating the electrical properties of metals extremely at cold temperatures. At that time, he found that *dc* resistivity of mercury wire suddenly drops to zero below 4.2 K. The search for new superconducting materials led to a slow increase in the highest known transition temperature T_c over the decades, reaching a plateau at 23 K with the discovery of superconductivity of Nb₃Ge by Gavaler [1]. In 1986, the discovery of superconductivity at ≈ 35 K in "LBCO" (LaBaCuO phase) by Bednorz and Muller [2] which opened the door for higher transition temperature superconductors and they were awarded Noble prize in 1987.

This discovery excited all researchers since it revealed that the oxides formed an unsuspected new class of superconducting materials with great potential other than large increase in T_c . Quickly, the $T_c \approx 90$ K reached with the discovery of RE123 (RE is rare earth elements) class of material [3, 4]. The achievement for more higher T_c were found in BiSCCO system [5] and TBCCO system [6]. In all these copper oxide planes form a common structural element, which is through to dominate the superconducting properties. Depending on the choice of stoichiometry, the crystallographic unit cell contains varying number of CuO₂ planes.

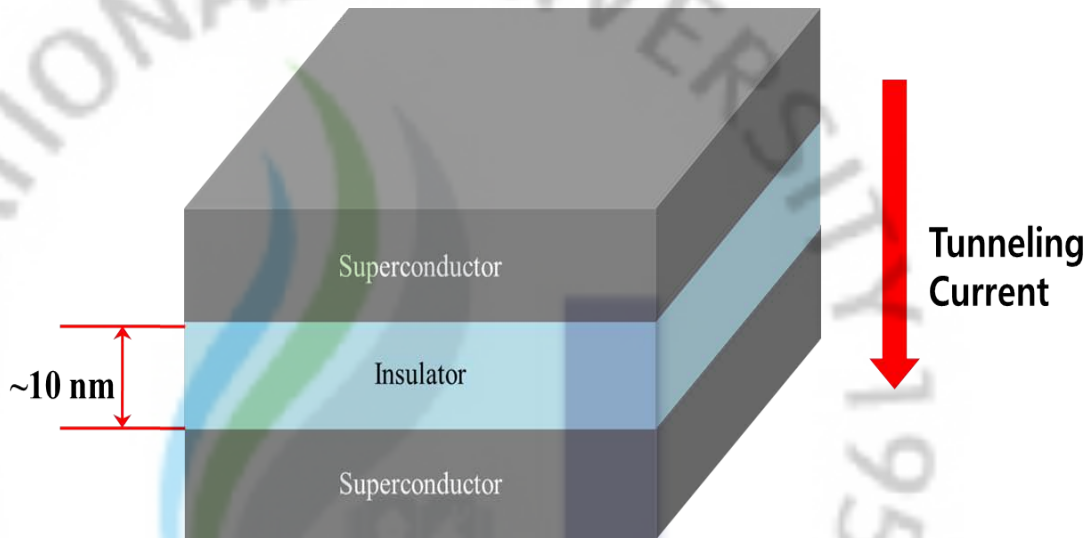


Fig. 1.1 The schematic of a Josephson junctions.

1.2 Josephson Junction

A Josephson effect [7] is a phenomenon when two superconductors are separated by thin insulator layer. Josephson predicted the occurrence of some unusual phenomenon in this situation a tunneling current at zero bias voltage. Shortly, this was observed experimentally and lead to the Nobel Prize to Josephson and Anderson. The structures which exhibits these phenomenon are known as Josephson junctions or weak links like Ref [8, 9, 10, 11, 12, 13]. Apart from these structures, in high T_c copper oxide materials (e.g. Bi-2212) *intrinsic* Josephson junctions (IJJs) tunneling occurs in the c -axis direction [14]. Figure 1.1 shows the schematic of a Josephson junction. The insulator barrier is so thin that cooper pairs tunnel through it.

In Josephson junction, the thin insulating layer allows the overlap of wave functions in two superconductors, resulting in the Cooper-pair tunneling. The current density in a superconductor can be described using the second Ginzburg-Landau (G-L) equation [15],

$$\mathbf{j} = -\frac{1}{2e\mu_0\lambda^2} (\hbar\nabla\theta + 2e\mathbf{A}) \quad (1.1)$$

where λ is the London penetration depth and \mathbf{A} is the vector potential. Equation 1.1 shows that the dc current in superconductor can be determined by the phase difference in absence of magnetic field. If a junction is biased with current and the Cooper pairs

tunnel through the tunneling barrier, the phase difference between two superconductors is defined by $\phi = \theta_1 - \theta_2$. This super current is define by the dc Josephson effect as

$$I_J = I_c \sin\phi \quad (1.2)$$

where I_c is the Josephson critical current. However the phase difference in an external magnetic field should be invariant under a gauge transformation of the vector and scalar potential. So the value of ϕ can be define as

$$\phi = \theta_1 - \theta_2 + \frac{2e}{\hbar} \int_2^1 \mathbf{A} \cdot d\mathbf{l} \quad (1.3)$$

When the junction is voltage biased, ϕ temporally oscillate according to the *ac* Josephson effect,

$$\partial_t \phi = \frac{2e}{\hbar} V = \frac{2\pi}{\Phi_0} V \quad (1.4)$$

$$\frac{2e}{\hbar} \approx 483.6 \text{ GHz/mV (or } \Phi_0 \text{ is } 2.067 \times 10^{-15} \text{ wb)} \quad (1.5)$$

where $\Phi_0 = h/2e$ is the flux quantum. The equation 1.2 and 1.4 predict that the oscillating current exists across the junction with the frequency $f_J = V/\Phi_0$ when a finite voltage V is biased across the junction. This properties provide the possibility of applications to the voltage standard devices and the high frequency devices such as oscillators and mixers [16].

1.3 Intrinsic Josephson junctions

In a layered high-temperature superconductor such as Bi-2212 which has highly anisotropic electric characteristics in the normal and superconducting states are a closely packed naturally grown Josephson junctions as shown in figure 1.2. The CuO_2 bilayer plane (0.3 nm in thickness) and the BiO-SrO layer (1.2 nm in thickness) act as the superconducting electrode and the tunneling barrier, respectively. The layered crystal forms a three dimensional superconductors by a weak Josephson coupling between the superconducting

layers and referred as *intrinsic Josephson junctions* (IJJs). The evidence for the existence of the Josephson junctions effect in the Bi-2212 intrinsic junctions has been revealed in the observation of the Fraunhofer diffraction pattern, Shapiro steps, Fiske steps, etc [17, 18, 19, 20].

1.4 Applications

Since the discovery of superconductor many potential applications are achieved. Table 1.1 is a summarized view in our knowledge based on superconductivity. A few of applications based on Josephson junction phenomenon are described in detail in following subsections.

1.4.1 Single Electron Transistor (SET)

A Josephson junction or a tunnel junction has a wide scope of application based on Coulomb blocking phenomenon such as a voltage standard, single electron transistor, etc [31, 32]. The Coulomb blockade refers the modifications of the tunneling current-voltage characteristics which occur in the junctions with capacitance sufficiently low so that the Coulomb charging energy $E_c = e^2/2C$ of a *single* electron is large enough to play a major role.

The simplest device in which the effect of Coulomb blockade can be observed is known as the single electron transistor (SET). It consists of two Josephson junctions or tunnel junctions sharing one common electrode with a low self-capacitance, known as the island. The electrical potential of the island can be tuned by a third electrode (the gate), capacitively coupled to the island. Figure 1.3 shows a schematic of SET along with a fabricated device in Bi-2212 single crystal whisker is taken from ref [21].

1.4.2 Terahertz Application

The Josephson effect has always been focused by the researcher because of its application in science and technology. The Josephson effect provides a unique principle to excite high-frequency electromagnetic (EM) wave in the single junctions or in arrays. The Josephson junctions can be used as the terahertz (THz) oscillator because of large superconducting

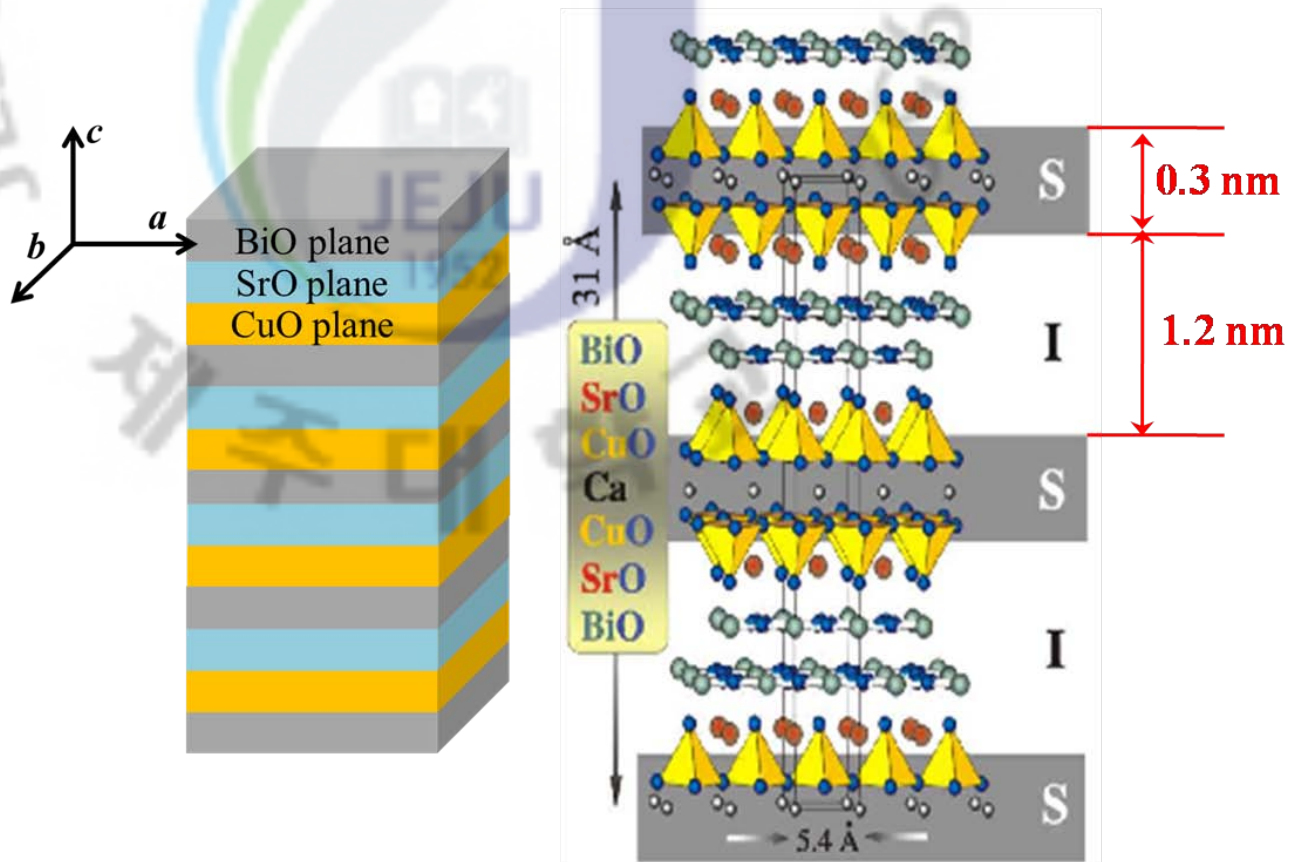


Fig. 1.2 Schematic of intrinsic Josephson junctions with axial representation.

Table 1.1 Various application of superconductivity

Concepts	Applications
R = 0 and high critical current density	Magnets for various application Passive microwave devices Interconnects in microelectronics Electrical energy transport by cables
Josephson tunneling	Microwave detectors and mixers In physical measurements (SQUIDs etc) Computers (fast logic and memory circuits) Plasma and space
High critical current at high critical magnetic field	Electrical power industry Plasma confinement (in high energy physics) In transport (levitation trains, MHD-propelled ships) Medicine (nuclear magnetic resonance tomography)

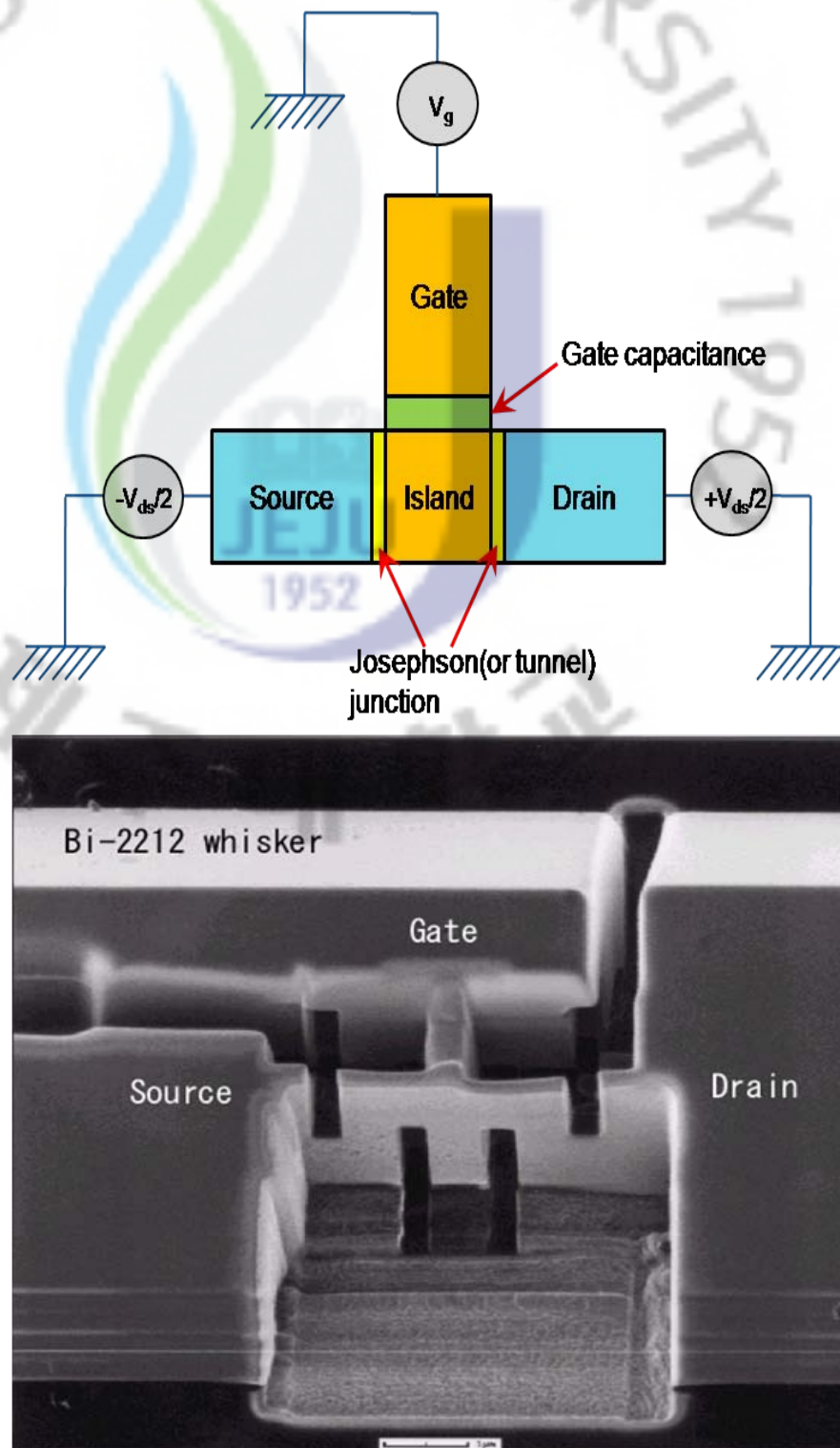


Fig. 1.3 Schematic of SET along with a fabricated device in Bi-2212 single crystal whisker taken from ref. 21.

gap as schematic shown in figure 1.4. Although the emission from a single junction is weak and many junctions can emit high enough power for different applications [22, 23, 24]. The solid-state THz radiation sources are useful for the application such as medicine, diagnostics, bio-science, ultrahigh-speed communication, environmental studies, security systems, and nondestructive and noninvasive sensing and imaging [25].

There are many studied have been done in high temperature layered superconductors. It has been challenging to synchronize all Josephson junctions in the stack. Various approaches for synchronizing the junctions have been studied such as applying a magnetic field to induce coherent Josephson vortex flow [26, 27, 28, 29, 30, 33] or putting the the device into a microwave cavity [34]. However the emitted power is in the range of pW only. Further a few of studies have shown a synchronized radiation of THz in the mesa of Bi-2212 of the power in range of μW . This synchronization was generated by a voltage biasing in c -axis in the absence of an external magnetic field. The EM emission takes place at the biasing voltage when the frequency determined by the ac Josephson relation equals to the fundamental cavity mode and corresponds to a half-wavelength of the plasma in the mesa. Synchronization of IJJs and mechanism behind the emission has given with coupling the cavity resonance with Josephson plasma frequency[35]. Wang et al. [36] presented the cavity resonance can't be the only mechanism to synchronize the IJJs and THz radiation. The hot spot (a region heated above the transition temperature) formed within the mesa give rise to coherent THz emission.

1.5 Summary

The quantum devices using Josephson junction phenomenon has been demonstrated. The application is focused on single electron transistor and terahertz devices. The low capacitance devices is demonstrated in this thesis. A part of this thesis also concentrated on the terahertz irradiation on submicron devices. These devices are expected to be next generation devices for science and technology.

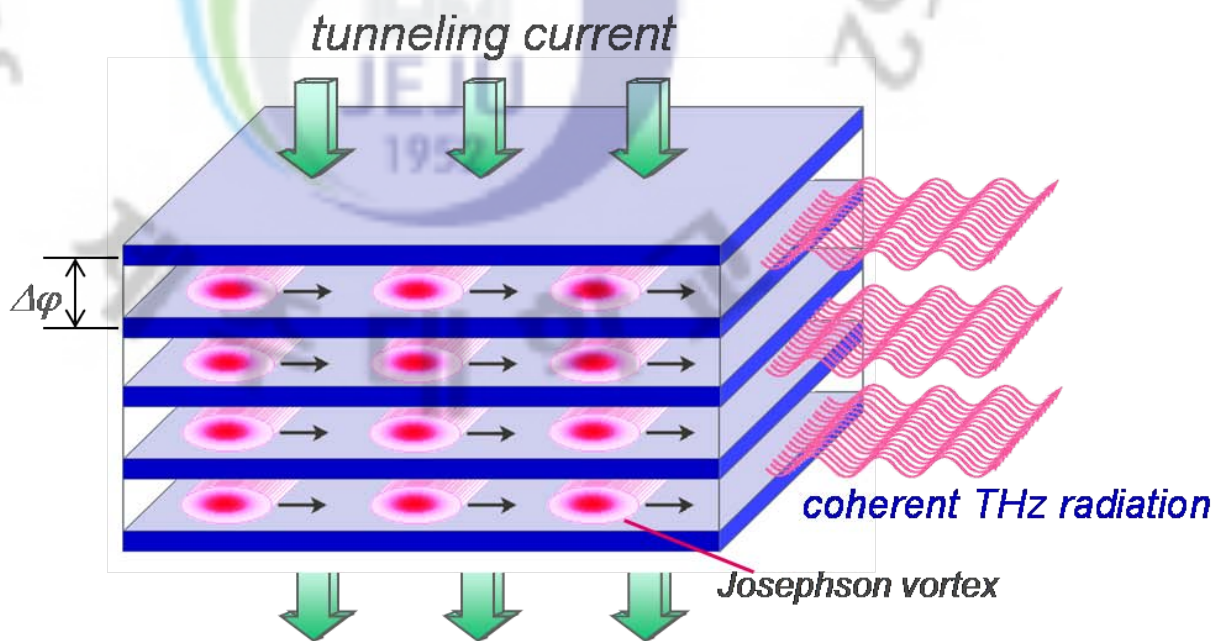


Fig. 1.4 Schematic of terahertz device using layered superconductor.
(Figure by Prof. H.-J. Lee, POSTECH.)

2. GROWTH OF BI-2212 SINGLE CRYSTAL WHISKERS

The thesis concern about the growth of $\text{Bi}_2\text{Sr}_2\text{CaCu}_2\text{O}_{8+\delta}$ (Bi-2212) single crystal whiskers. We have succeeded in the growth of superconducting Bi-2212 single crystal whiskers with a Te-doped method. We use a Te-doped precursor with the mixed pure powders Bi_2O_3 , SrCO_3 , CuO and TeO_2 into the ratios of $\text{Bi}_2\text{Sr}_2\text{Ca}_2\text{Cu}_{2.5}\text{Te}_{0.5}\text{O}_x$. Bi-2212 single crystal whiskers have grown through the pellet surface 2-4 mm in length and 20-100 μm in width. Characteristics of whiskers were investigated by the resistance - temperature (R - T), X-ray diffraction (XRD) and current - voltage (I - V) measurements. The R - T characteristics in ab -plane of the whiskers showed that their $T_{c,on}$ and $T_{c,end}$ were about 106 K and 75 K, respectively and confirmed that the whiskers had Bi-2212 single crystal phase by XRD pattern. The I - V curves showed multi-branch structures of intrinsic Josephson junctions (IJJs) as evidence of c -axis transport characteristics.

2.1 Introduction

Since the discovery of Bi-based high- T_c superconductors (HTS) $\text{Bi}_2\text{Sr}_2\text{CaCu}_2\text{O}_{8+\delta}$ (Bi-2212), much effort has been focused on the growth of their single crystals [5, 37, 38, 39, 40, 41, 42]. Recent developments suggest that whiskers might be used in the fabrication of new electronic devices using intrinsic Josephson effects (IJE) and related phenomena, such as Josephson plasma oscillations [43, 44]. Stacked junctions have been fabricated by using Bi-2212 whiskers and are thought to be prospective candidates for high frequency applications of the IJE [45, 46].

When we use single crystal whiskers for fabrication of intrinsic Josephson junctions

(IJJs) using layered structures, single phase transition of critical temperature (T_c) without any crystal defects is one of the most important factors for controlling the IJJs characteristics. Although a few of growing methods were introduced, the reproducible electrical transport characteristics of single phase transition were not studied in detail.

In this chapter, we investigate the growing methods and growing conditions of Bi-2212 single crystal whiskers for using a base material of HTS devices with high quality and good crystallinity.

2.2 The growth process

The starting materials were prepared by mixing and grinding pure powders of Bi_2O_3 , SrCO_3 , CuO and TeO_2 in the ratios of $Bi : Sr : Ca : Cu : Te = 2 : 2 : 2 : 2.5 : 0.5$. The mixed powders were calcined in air and ground three times at 760-820 °C. The calcined powders were pressed at 60 kN into pellets 10 mm in diameter and 2-3 mm in thickness. The pellets were set in a pure alumina boat and heat treated at 870 °C for 100 h in flowing oxygen at rates of 150-500 ml/min.

The phases of crystal structures of Bi-based whiskers were investigated with X-ray diffraction (XRD) measurements. Figure 2.1 shows the heat treatment process for single crystal whisker growth. Prior to that, the sample was heat treated at 880 °C for 15 min to promote partial melting as shown in the inset of figure 2.1. During the process we used an oxygen atmosphere with a constant flow of 150 mL/min. The whiskers were grown on the surface of pellet, being of various dimensions in length (0.5 to 3 mm), width (10 to 30 μm) and thickness (0.5 to 3 μm).

2.3 Results and discussion

Figure 2.2 shows the Bi-2212 whiskers grown from a pellet. Those whiskers grow through the pellet surface in the range of 2-5 mm in length and 20-100 μm in width.

The growth conditions of Bi-based whiskers were summarized in table 2.1. The Te content is one of the important factors in whisker growth. We fixed the Te contents to be 0.5 as shown in Ref. [47]. In our experience, the next important factor is Ca and Cu contents. The optimal contents are 2.0 and 2.5 for Bi-2212 single crystal whisker growth.

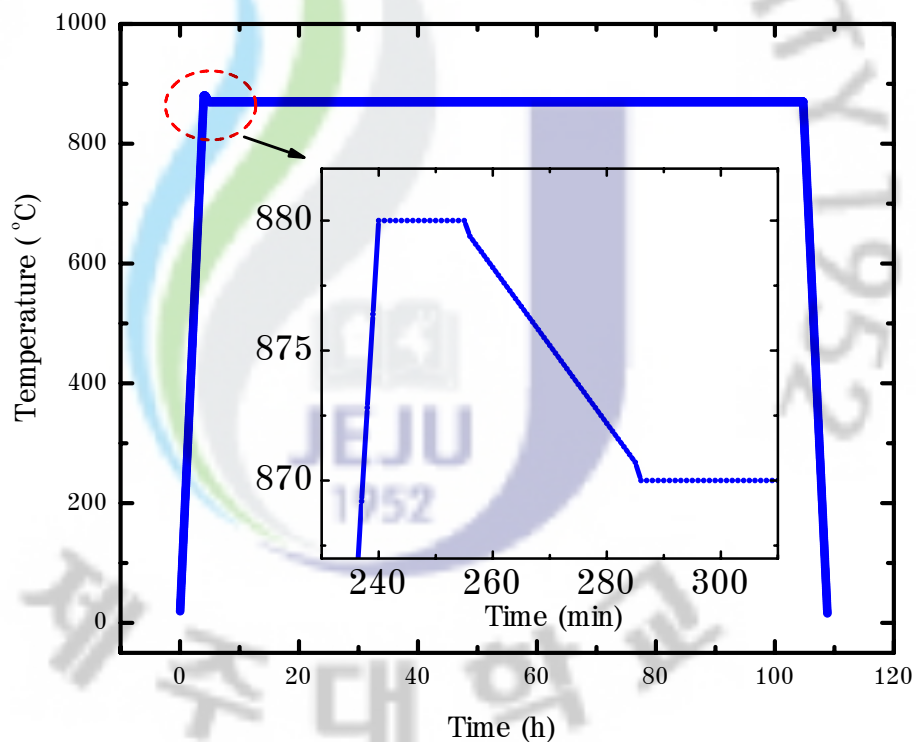


Fig. 2.1 The heat treatment process to grow Bi-2212 single crystal whiskers.

Table 2.1 Typical conditions for whisker growth: the nominal compositions of precursors and oxygen flow rates

$\text{Bi}_2\text{Sr}_2\text{Ca}_u\text{Cu}_v\text{Te}_w\text{O}_x$			O_2 (ml/min)	T_{max} °C	t_{max} (h)	Length L_a (mm)	Phase
u	v	w					
1.0	2.0	0.5	150	875	100	No Whisker	
2.0	2.5	0.5	150	870	100	2-3	2212
2.0	2.5	0.5	300	870	100	3-4	2212
2.0	2.5	0.5	500	870	100	4-5	2212

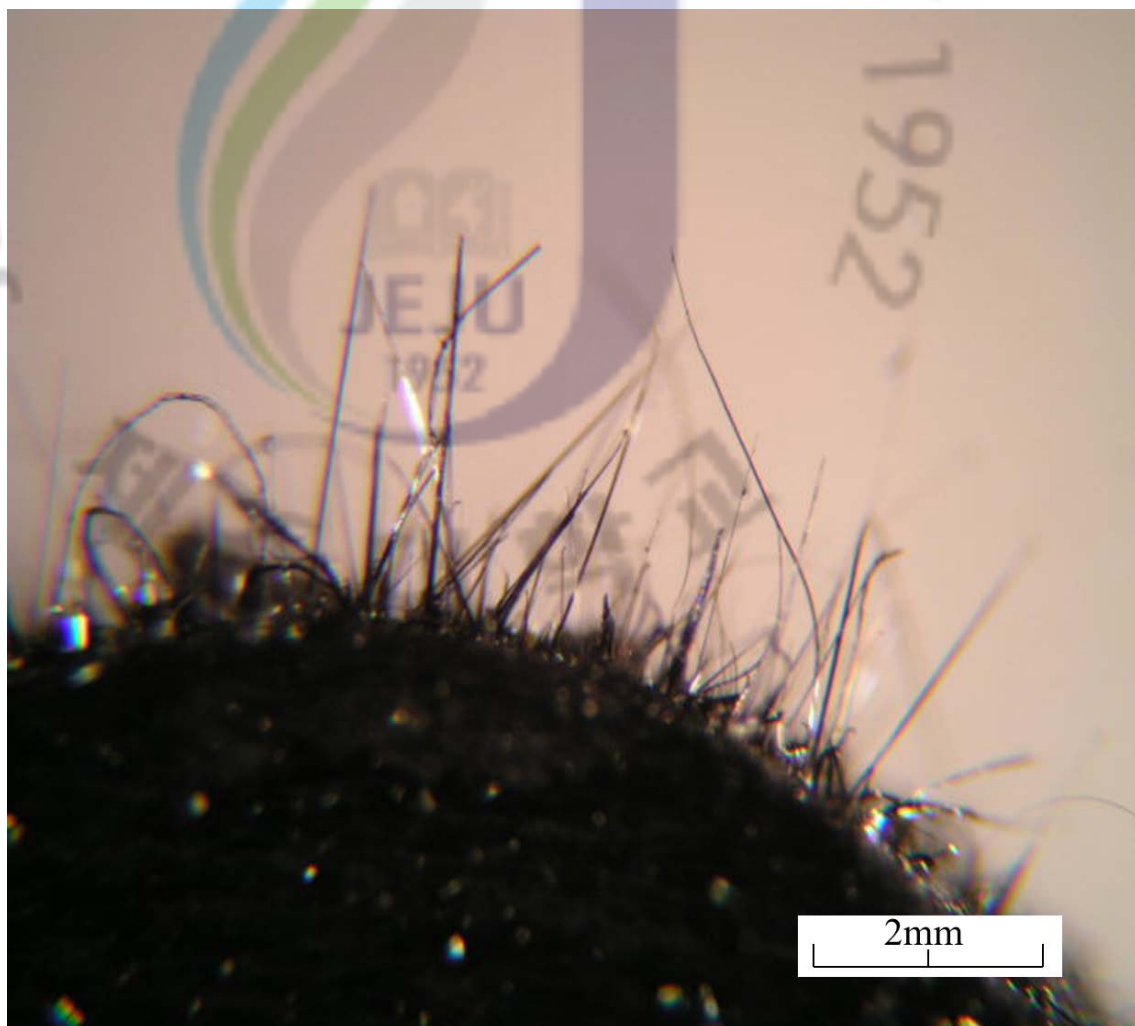


Fig. 2.2 An optical microscope image of as grown single crystal whiskers on the precursor pellet.

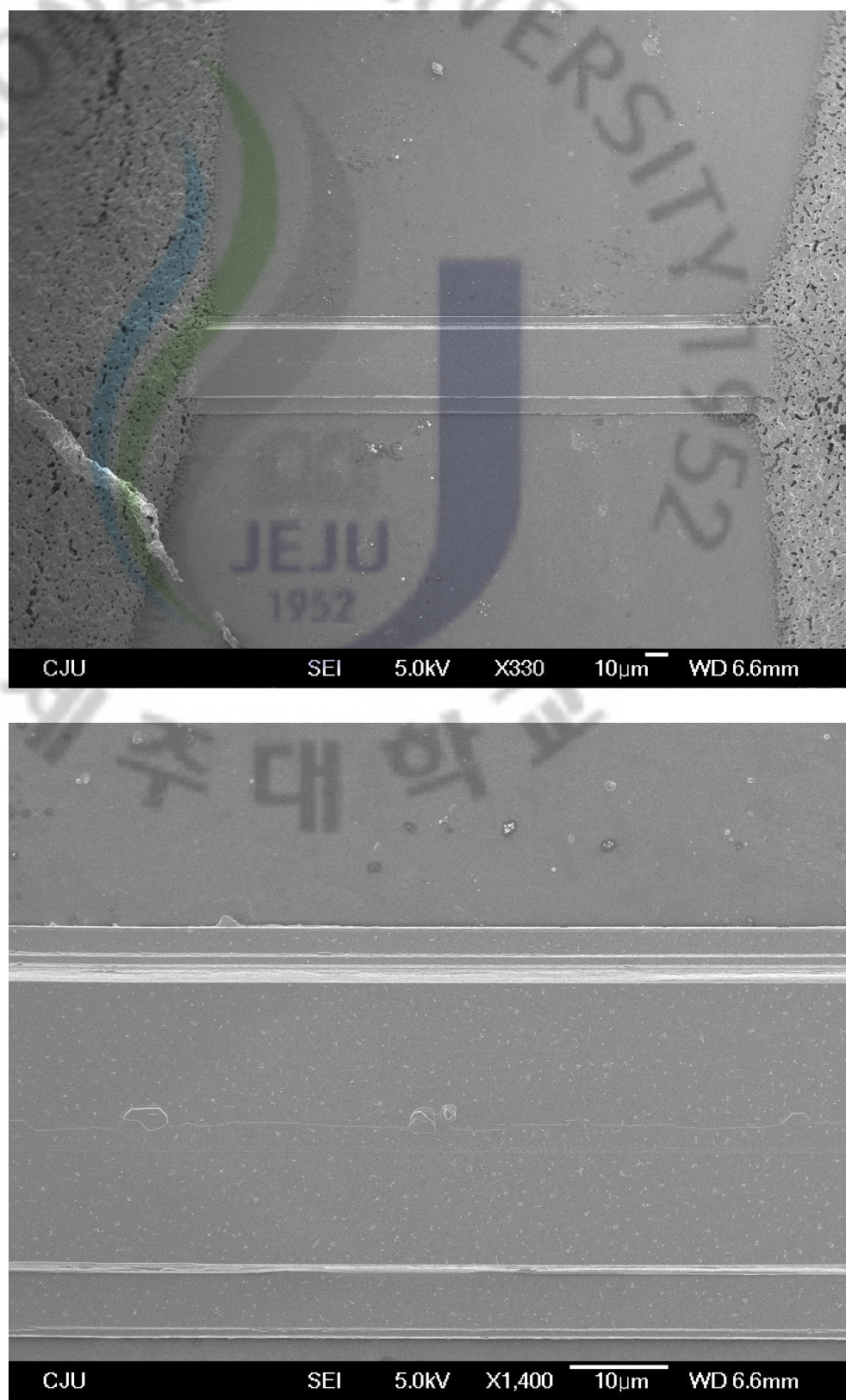


Fig. 2.3 A SEM image to see the smooth surface of Bi-2212 single crystal whisker.

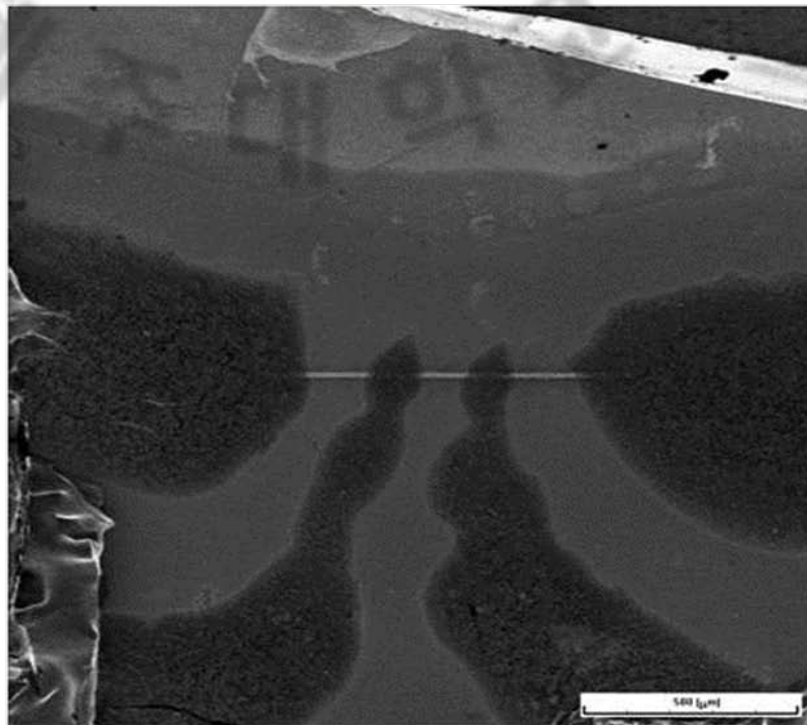
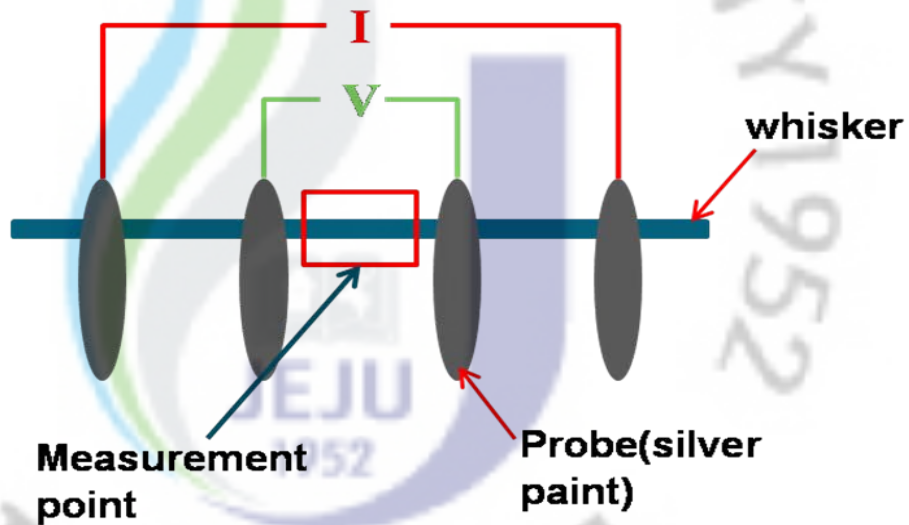


Fig. 2.4 Four probe configuration for electrical characterizations.

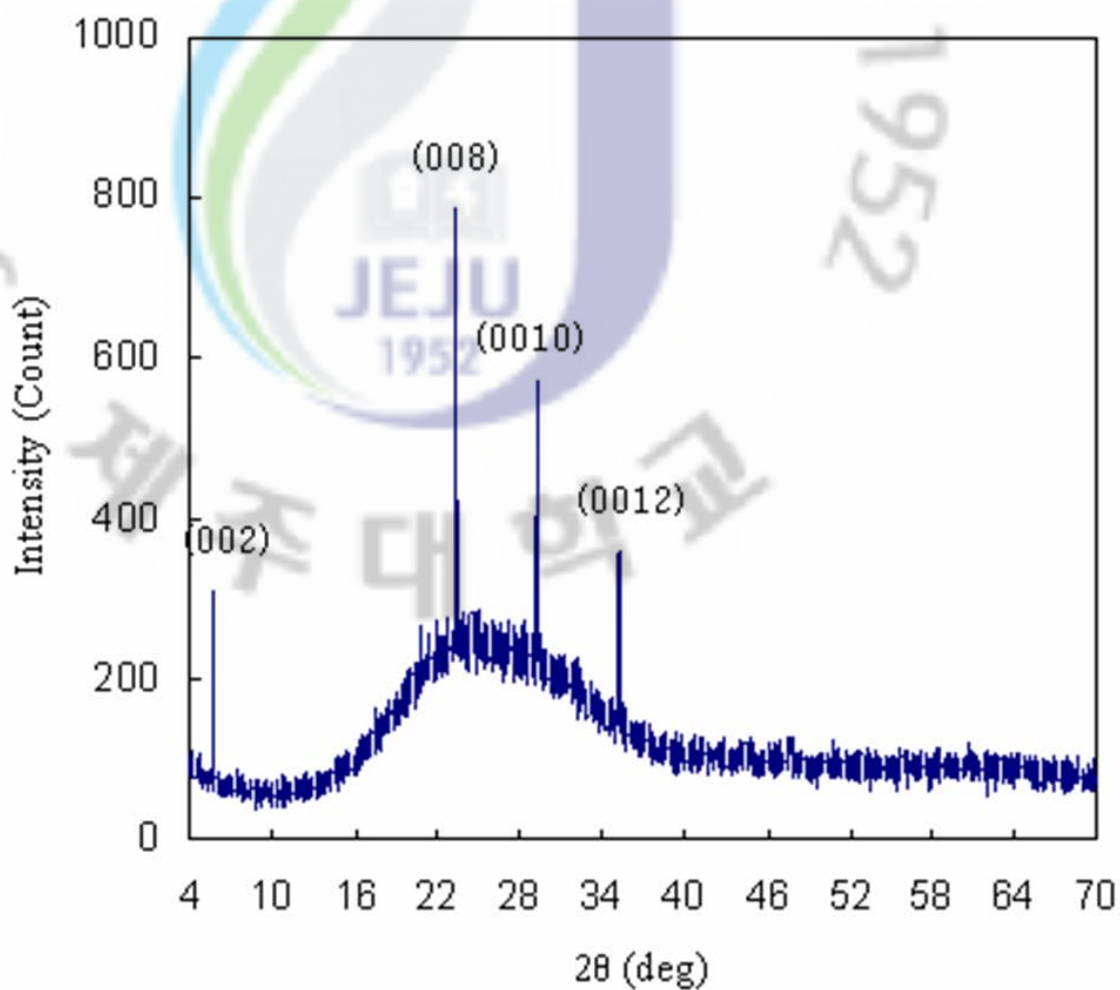


Fig. 2.5 X-ray diffraction patterns of as-grown Bi-based whiskers prepared at 870 °C for 100 h in oxygen flow rates of 150 ml/min.

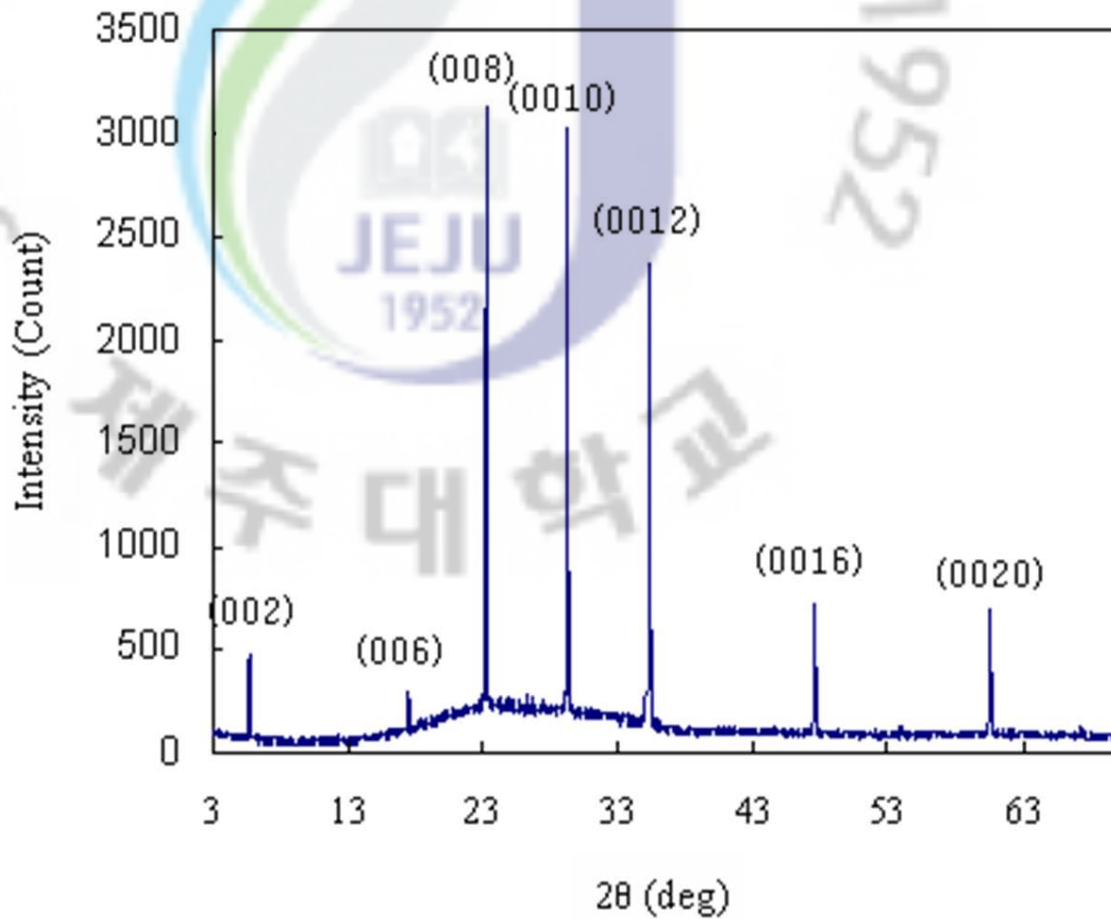


Fig. 2.6 X-ray diffraction patterns of as-grown Bi-based whiskers prepared at 870 °C for 100 h in oxygen flow rates of 300 ml/min.

Those whiskers of stoichiometric Ca and Cu contents of 1.0 and 2.0 did not grow. The lengths in a -axis (L_a) of grown whiskers increased when oxygen flow rates were increased from 150 ml/min to 500 ml/min.

The magnified SEM image of a whisker indicates smooth surface of whisker and high in quality, see Figure 2.3. All four electrodes were prepared with silver paint on a whisker and attached on an MgO substrate as shown in figure 2.4. The sample was annealed at 450 °C for 5 min in presence of oxygen to reduce the contact resistance between whisker and silver paint. The smooth surface reflects good quality of the whisker.

Figure 2.5 shows the XRD pattern of as-grown whiskers prepared at the growth temperature of 870 °C for 100 h in flowing oxygen. Only $(0\ 0\ l)$ XRD peaks were observed, which corresponds to the Bi-2212 phase with its c -axis perpendicular to the plane of the whisker. In addition, we found that the FWHM of the $(0\ 0\ 8)$ XRD peak was about 0.06°, which corresponds to the limit of the resolution of our XRD instrument. So the true half width of the $(0\ 0\ 8)$ XRD peak is likely to be less than 0.06°. We could observe the XRD pattern of a c -axis oriented Bi-based whisker with single phase of the Bi-2212 crystal structure. Oxygen flow rates were 150 ml/min in figure 2.5 and 300 ml/min in figure 2.6. From the peak intensity of XRD patterns, we found that the whiskers show the better crystallinity when oxygen flow rates are the larger.

2.4 Summary

The $\text{Bi}_2\text{Sr}_2\text{CaCu}_2\text{O}_{8+\delta}$ (Bi-2212) superconducting single crystal whiskers have grown successfully with a Te-doped method, although the Bi-2223 phase did not disappeared completely. The whiskers with lengths of about 2-3 mm were prepared at the growth temperature of 870 °C in flowing oxygen at the flow rate of about 150 ml/min for 100 h. The lengths in a -axis of grown whiskers were longer and the crystallinity of whisker Bi-2212 single crystal phase was better when oxygen flow rates were larger. Thus, the oxygen flow rate was one of the most important parameters for growing high quality single crystal whisker.

3. THREE-DIMENSIONAL FOCUSED ION BEAM MILLING TECHNIQUE

3.1 Introduction

Various fabrication methods have been applied to developed high T_c superconducting devices [48, 49]. The fabrication of tunneling devices of Josephson junctions in the layered high T_c superconductors are needed a special attention because of a perfect stacked structure with a very small lateral size compared with the Josephson penetration depth ($\lambda_J = \gamma d$) [50, 51, 52], where $\gamma = \lambda_c/\lambda_{ab}$ is the London penetration depth anisotropy ratio and d is interlayer spacing [53].

The three dimensional focused ion beam (3D-FIB) milling method is a reliable and versatile technique for the fabrication of nanoscale Josephson junctions in single crystal whiskers. In a FIB, a finely focused beam of gallium ions is used. As the beam rasters across the surface, an image of nanoscale resolution can be built up using secondary electrons when the FIB is operated at low beam currents. The FIB can also be operated at high beam currents for site specific sputtering or milling.

3.2 The Focused Ion Beam

The FIB system has introduced in late 1980s and become an essential tool in the microelectronics industry. The principle of operation is similar to a Scanning Electron Microscope (SEM). The major difference is that in place of an electron source a gallium liquid metal source is used. This helps both imaging and milling of the sample. In addition, deposition of extra material can be achieved by ion beam-induced decomposition of an organometallic gas. This versatile instrument allows faulty circuits to be both inspected and modified.



Fig. 3.1 A picture of FIB machine (SII NanoTechnology SMI2050) in Research Institute of Center (RIC).

Recent researches have exploited the ability of this instrument to create sub-micron scale features without resorting to complex and time-consuming techniques.

3.2.1 Fundamental Operating Principle of FIB

At top of the ion source chamber, a liquid metal ion source (LMIS) is placed. A high vacuum ($= 6 \times 10^{-5}$ Pa) environment is maintained in the ion source chamber to avoid ion beam interference with gas molecules. An acceleration voltage is applied to ions to make ions pass through the ion column and move toward to the main chamber. The ions are focused to the fine ion beam by the aperture and electrostatic lenses in the ion column while passing through the ion column.

A sample is fixed at the sample holder which is located in the main chamber (base pressure 5×10^{-4} Pa). When ion beam is irradiated, the secondary electron and the secondary ions are generated from the specimen surface. The secondary electrons or ions are converted into the electric signals and the two dimensional distribution of these signals is displayed as a microscope image. The atoms of the surface materials are expelled when ion beam is irradiated to the specimen. This phenomenon used as etching to remove materials from the sample. When the irradiating ions beams while spraying a specific compound gas on the specimen surface, the solid elements of gas are adhered to the specimen surface and accumulated. This phenomenon used as deposition of the material to the specimen surface.

3.3 Fabrication of Josephson junctions

In our laboratory the FIB machine (SII NanoTechnology SMI2050) can be used for etching as well as deposition of the materials. A picture of FIB machine is shown in figure 3.1. The FIB machine has a freedom of tilting and rotating the sample stage up to 60° and 360° respectively. A sample stage that itself inclined by 60° with respect to the direction of the ion beam is used for 3-D milling. The detailed fabrication process is shown in figure 3.2.

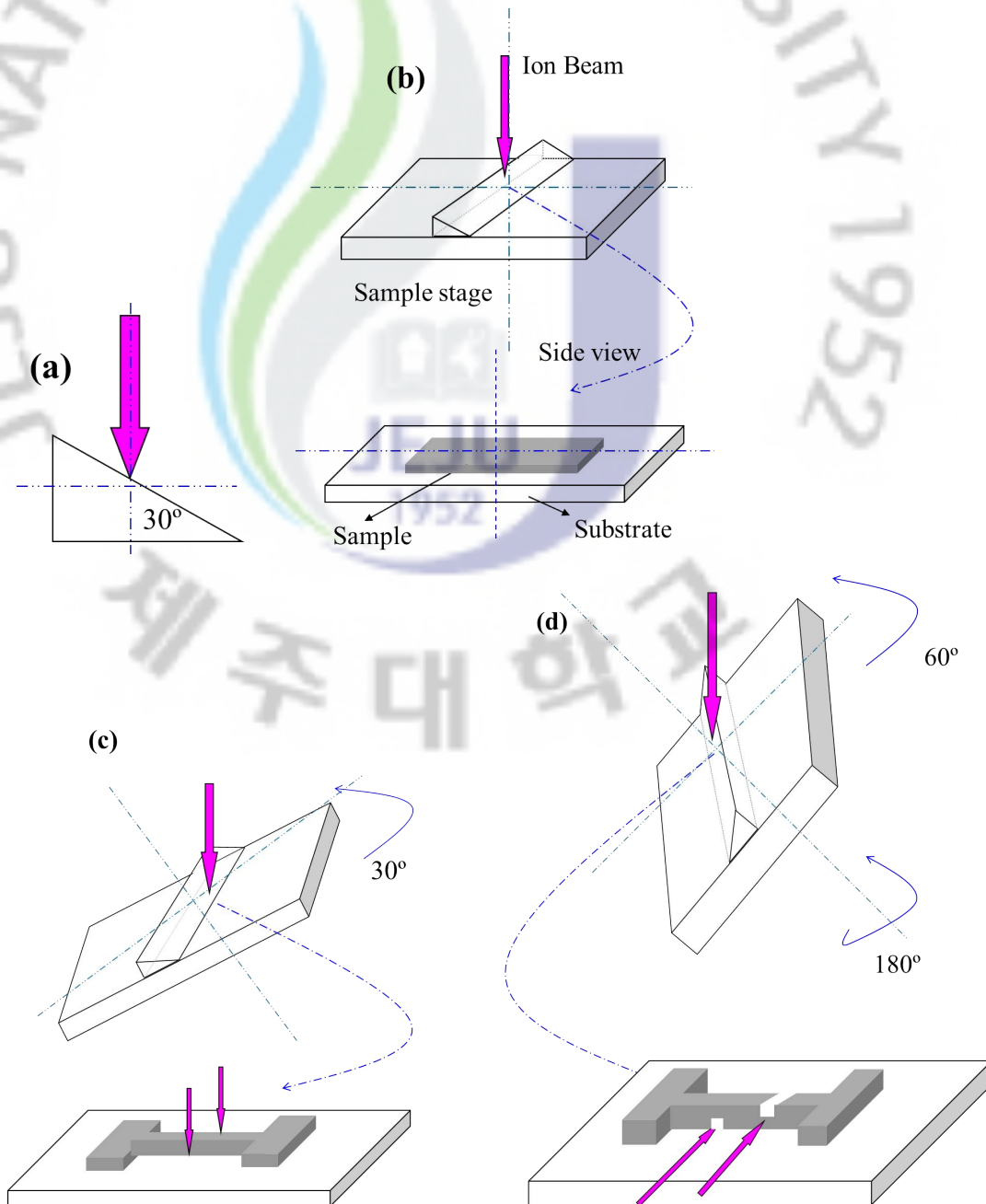


Fig. 3.2 The steps of fabrication process of Josephson junctions by FIB. (a) The inclined sample stage where we mount a sample. (b) A side view of as mounted sample on sample stage. (c) The first etching process to mill junctions in-plane area. (d) The final etching in two grooves.

In the first step we milled sample in bridge pattern from the top direction. As shown in figure 3.2 (c), we tilted the sample stage by 30° so that the in-plane of sample was set to be perpendicular to the ion beam and the sample was milled in bridge pattern with desired junction area.

We turned sample stage back to the initial orientation and rotated it by 180° so that the incline plane was set to be 60° with respect to the ion beam. We then tilted sample stage by 60° so that the thickness of the sample was set to be perpendicular to the ion beam and two grooves of similar depths were etched the whole length and the distance between grooves was set according to the required junction size [54].

3.4 Summary

The fabrication process is used to fabricate intrinsic Josephson junctions in $\text{Bi}_2\text{Sr}_2\text{CaCu}_2\text{O}_{8+\delta}$ (Bi-2212) single crystal whiskers. The results in this thesis shows that the intrinsic Josephson junction devices have been fabricated successfully using three dimensional focused ion beam milling technique.

4. INTRINSIC JOSEPHSON JUNCTIONS STACK OF BI-2212

4.1 Introduction

Since the discovery of Bi-based high- T_c superconductors, much effort has been given to grow single crystal. Single crystal whiskers are always be in focused due to perfect crystallinity and show unique properties in an ultra small size. In Bi-based single crystal whisker, the conducting CuO_2 planes are separated by insulating BiO-SrO layer [55]. This layered phenomenon gives high anisotropy to Bi-based single crystal whisker. Bi-based single crystal whisker is a naturally grown intrinsic Josephson junctions (IJJs). These junctions are attractive because the anomalous nonlinear current-voltage (I - V) characteristics along the c -axis and a series of several hundred Josephson junctions can be easily obtained [56].

The junctions are considered to be a one-dimensional array of Josephson junctions in the stack. IJJs are attractive objects for studying the Josephson effect. There are three compounds in the Bi-family high temperature superconductors, differing in the type of planar CuO_2 layers; single-layered $\text{Bi}_2\text{Sr}_2\text{CuO}_{6+\delta}$ (Bi-2201) single crystal, double-layered $\text{Bi}_2\text{Sr}_2\text{CaCu}_2\text{O}_{8+\delta}$ (Bi-2212) single crystal, and triple-layered $\text{Bi}_2\text{Sr}_2\text{Ca}_2\text{Cu}_3\text{O}_{10+\delta}$ (Bi-2223) single crystal [57]. The compounds have transition temperature (T_c) about 20 K, 85 K, and 110 K for Bi-2201, Bi-2212, and Bi-2223, respectively. However Bi-2223 has highest T_c in this family but the phase is not stable and difficult to grow. In our study, we have used Bi-2212 single crystal whiskers which has stable phase and high T_c .

The conducting CuO layers are separated by insulating BiO-SrO layers. The characteristics of IJJs can be measured by flowing current in vertical direction as shown in

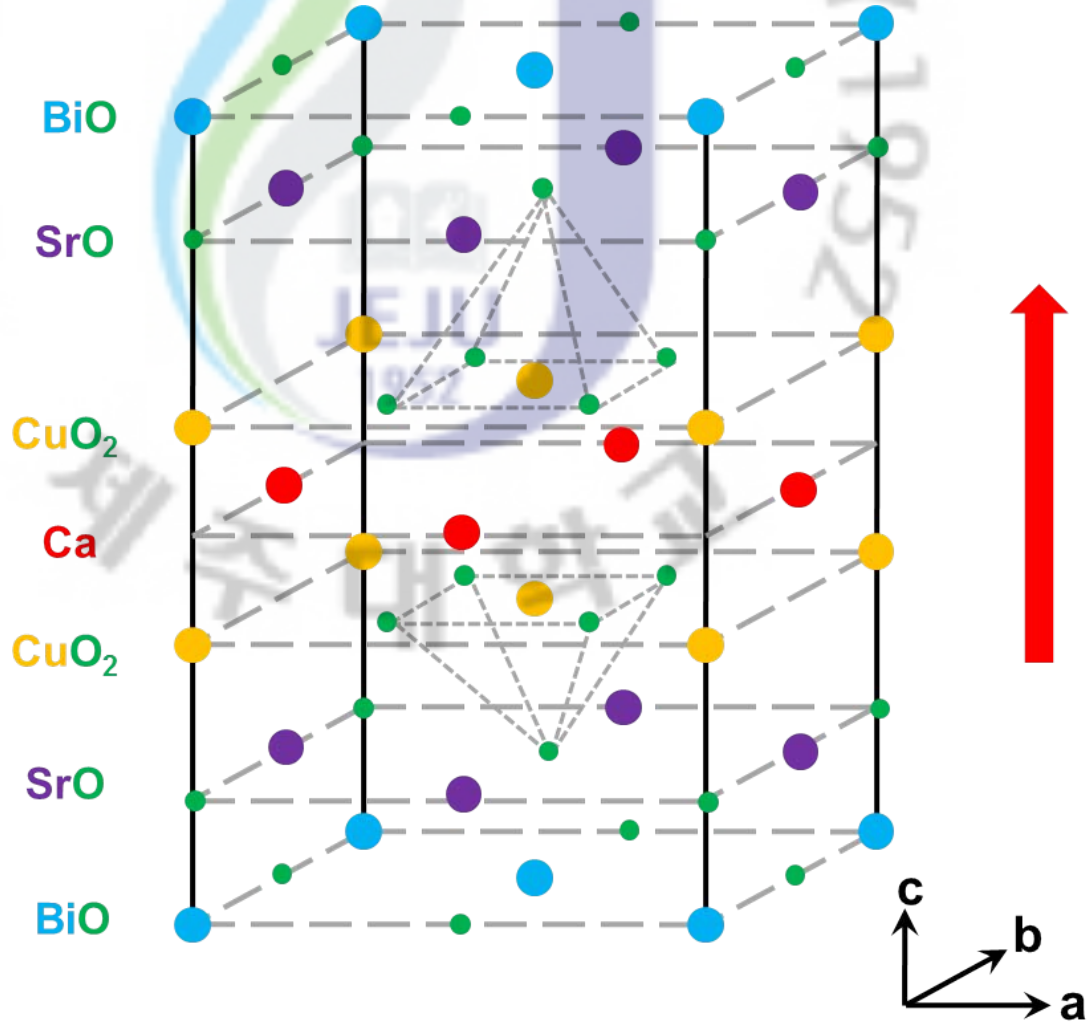


Fig. 4.1 The red arrow indicates the direction of current to measure the characteristics of IJJs in Bi-2212 single crystal whiskers.

figure 4.1. The red arrow in figure 4.1 shows the direction of current.

4.2 Experimental details

Bi-2212 single crystal whiskers used in this study were grown by solid state reaction method as described in chapter 2. A Bi-2212 whisker was mounted on MgO substrate. The silver paint was used to make four electrodes for electrical characterization. To minimize contact resistance, the sample was annealed for 5 minutes at 450°C in presence of oxygen. The stacks were fabricated using three dimensional focused ion beam (3-D FIB) milling process. The 3-D FIB machine (SII NanoTechnology SMI2050) is operating with a gallium ion beam of energy 30 keV and beam current from 1 pA to 20 nA. The detailed fabrication process is described elsewhere [54, 58]. Briefly in this process, the FIB machine has a freedom of tilting and rotating the sample stage up to 60° and 360° respectively. We used a sample stage that itself inclined by 60° with respect to the direction of the ion beam. We tilted the sample stage by 30° so that the *ab*-plane of sample was set to be perpendicular to the ion beam and the sample was milled along the *ab*-plane. We turned sample stage back to the initial orientation and rotated it by 180° so that the incline plane was set to be 60° with respect to the ion beam. We then tilted sample stage by 60° so that the *c*-axis of the sample was set to be perpendicular to the ion beam and the sample was milled along the *c*-axis. The Bi-2212 single crystal whisker was then etched the *ab*-plane. With the precise control in 3-D FIB fabrication process, we were able to achieve the height of stack about 100 nm. In this study, the whisker was annealed before the 3-D FIB fabrication process to avoid Ga⁺ ion contamination. The measurement were done at 10 K. The dimensions of the stacks are 2 μm × 2 μm with the height of 100 nm.

Keithley 2182A nano voltmeter and Keithley 6221 AC & DC current source were used to measure resistance-temperature (*R-T*) characteristics and current-voltage (*I-V*) characteristics for different in-plane stacks using conventional four probe technique in current biasing mode. The low pass filters were used in signal line to reduce the external noise at room temperature.

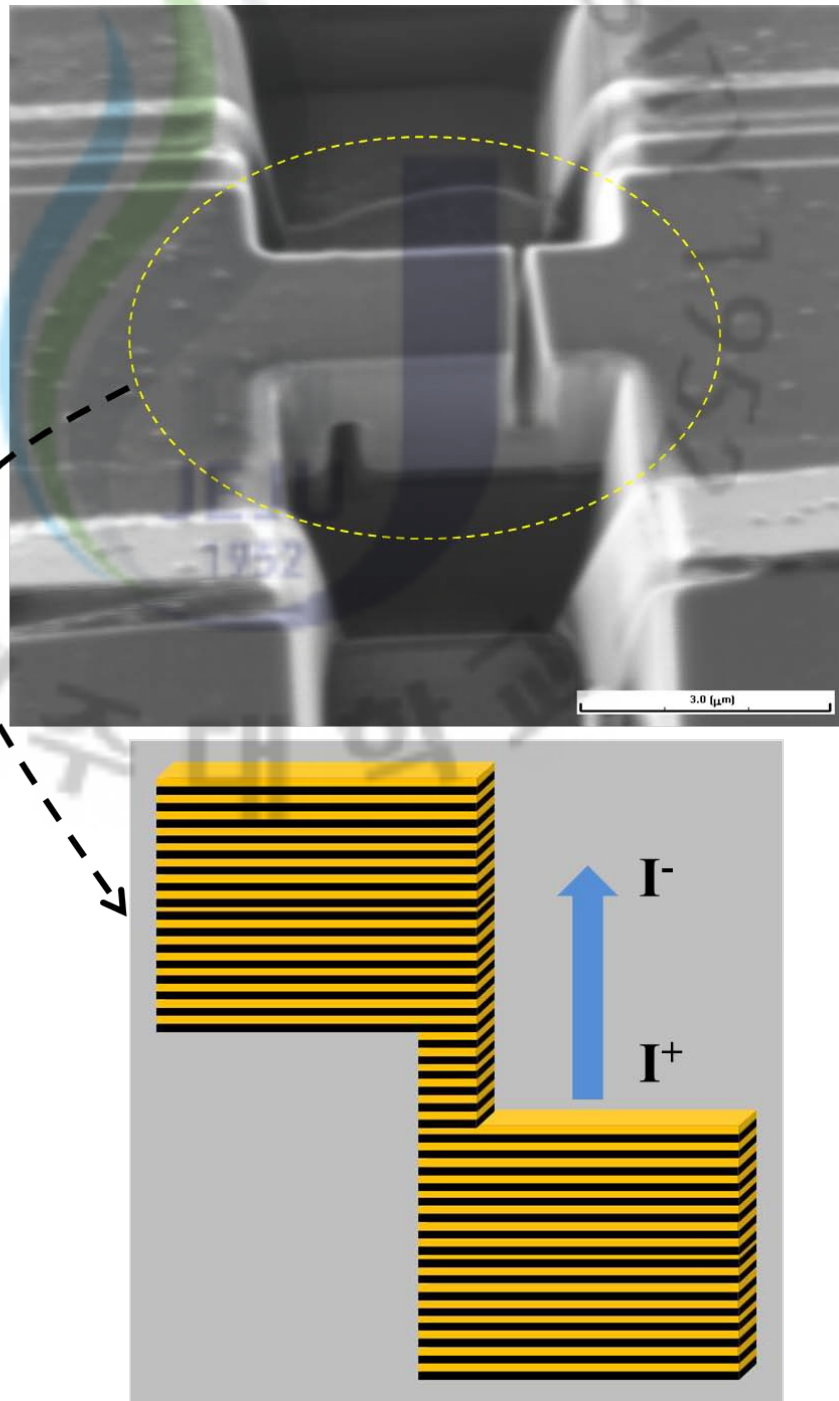


Fig. 4.2 FIB image of stack and schematic of the IJJs configuration in the stack. The blue arrow indicates the direction of current flow which is along the IJJs.

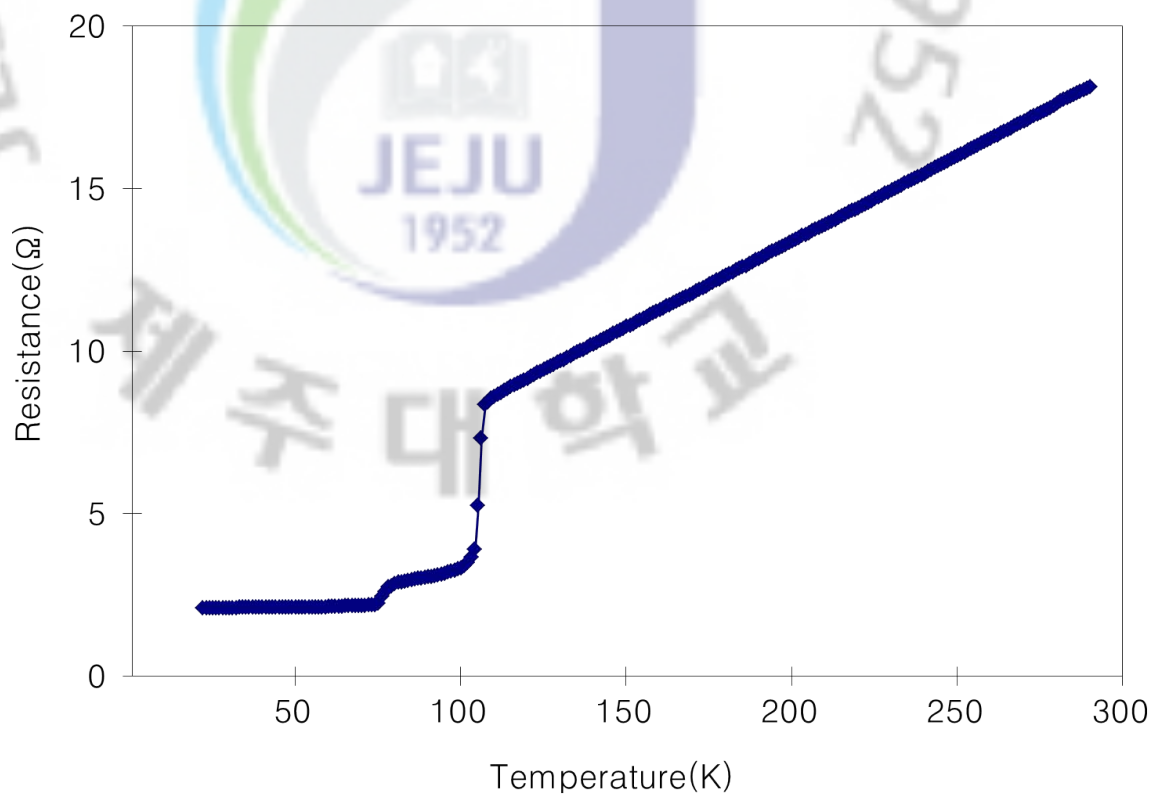


Fig. 4.3 The resistance vs. temperature characteristics of the stack in *ab*-plane.

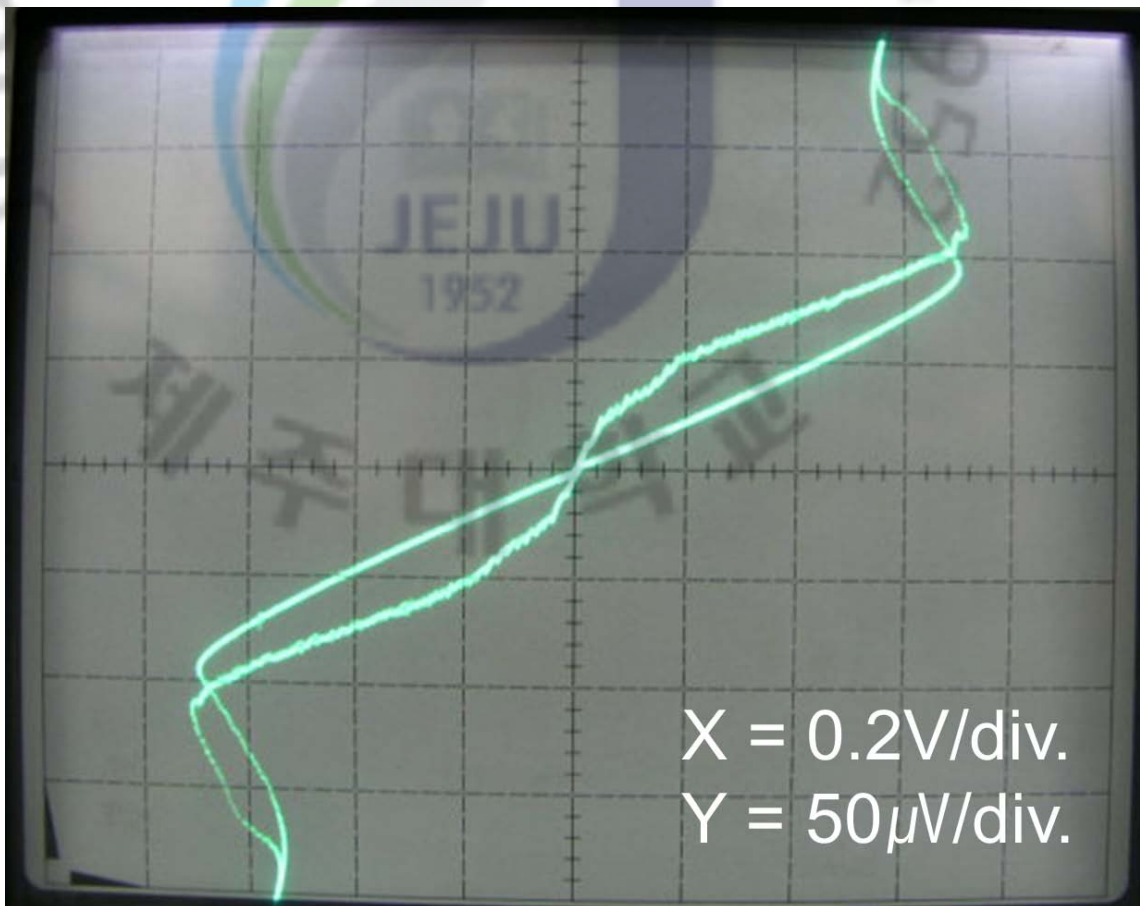


Fig. 4.4 The current (I) vs. voltage (V) characteristics of the stack at 10 K.

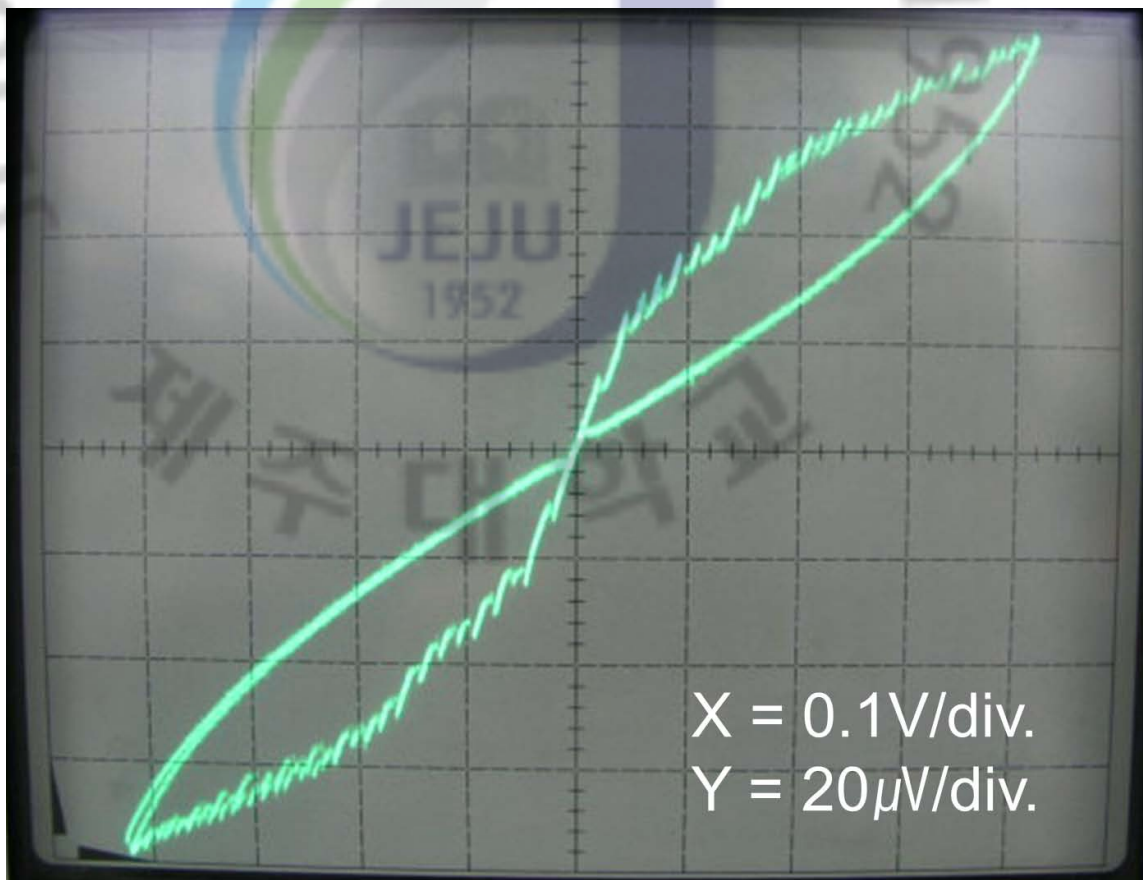


Fig. 4.5 The current (I) vs. voltage (V) characteristics at low biasing of the stack at 10 K.

4.3 Results and discussion

An FIB image of a stack with the scale bar of $3 \mu\text{m}$ is shown in figure 4.2 along with the schematic of the stack. The dimensions of the stack are $2 \mu\text{m} \times 2 \mu\text{m}$ with height of 200 nm. Conducting CuO planes are sandwiched by insulating BiO-SrO planes which work as IJJs [55]. These IJJs are arranged in series of an array in Bi-2212. The schematic of stack is also shown in figure 4.2. The spacing between these elementary IJJs is about 1.5 nm. The number of elementary IJJs ($N = z/1.5$) can be calculated from the height (z) of the stack [59, 60]. Therefore, the stack has approximately 130 elementary IJJs.

Figure 4.3 shows *ab*-plane *R-T* characteristics of a whisker grown at 870°C for 100 h in flowing oxygen. The whisker showed a metallic temperature dependence of resistance in the normal state above T_c . The *R-T* curves in *ab*-plane showed two phase transitions between $T_{c,on}$ of 106 K and $T_{c,end}$ of 75 K which reflect the characteristics of Bi-2223 and Bi-2212, respectively. This result indicates that the quantity of Bi-2223 phase is small and may be distributed as small defects like dislocation.

Figure 4.4 shows the typical *I-V* characteristics of a stacked junction. A well-defined gap voltage is clearly seen in *I-V* curves. The value of each voltage gap is approximately 20 mV. The regular intervals of the voltage jumps are thought to be due to the current paths being parallel to the *c*-axis. The origin, low quality or ion-beam damage, of the slanted *I-V* curves at low biases is not clear. We observed the slanted *I-V* curves at low bias regions shown in figure 4.5.

For the stacked junctions, we observe *S*-shaped *I-V* characteristics at $V \approx V_g$ due to quasiparticle injection or selfheating [45]. A clear gap structure is seen in the *I-V* characteristics at $V_g \approx 0.6 \text{ V}$, which corresponds to the superconducting gap for *N* elementary junctions connected in series. From the gap value of 20 mV for elementary junctions, we find the number of elementary is approximately 30 elementary layers. The observation of multi-branched structures indicates that the grown whisker behaves as an interlayer-tunneling stack of series array and can be used as new electronic device using the IJE.

The existence of the Bi-2223 phase in *R-T* characteristics may be due to a disproportionate reaction of the Bi-2212 to form the 2223 [63] and/or to a precipitated Bi-2223

phase from a partially melted phase [64]. Also, the supply of atomic species such as Ca, Sr, Cu, and O into the 2212 phase induces an edge location that leads to the Bi-2223 phase [65], the formation of the Bi-2223 phase being easier at a lower oxygen partial pressure [66]. These mechanisms suggest that the 2223 phase is produced through the Bi-2212 phase which acts as a precursor for the 2223 phase [67]. Therefore, control of the composition of the calcined powder and of the oxygen pressure could be important factors to obtain pure single phase Bi-2212 whiskers.

4.4 Summary

In conclusion, we have fabricated stack of intrinsic Josephson junctions of Bi-2212 whiskers of different of in-plane area $2 \mu\text{m} \times 2 \mu\text{m}$. The R - T curves in ab -plane showed two phase transitions between $T_{c,on}$ of 106 K and $T_{c,end}$ of 75 K which reflect the characteristics of Bi-2223 and Bi-2212, respectively. While in c -axis the transition temperature is about 77 K. The observation of multi-branched structures indicates that the grown whisker can work as an interlayer-tunneling stack of series array and can be used as new electronic devices using IJE.

5. CONCLUSIONS

The single-crystal whiskers of $\text{Bi}_2\text{Sr}_2\text{CaCu}_2\text{O}_{8+\delta}$ (Bi-2212) have attracted much attention because they have perfect crystallinity, are free of dislocations, show peculiar dimensions with extremely small cross-sections, and have excellent superconducting properties. The developments suggest that whiskers might be used in the fabrication of new electronic devices using intrinsic Josephson junctions and related phenomena, such as Josephson plasma oscillations. Stacked junctions have been fabricated by using Bi-2212 whiskers and are thought to be prospective candidates for high-frequency applications of the intrinsic Josephson effect.

We have succeeded in the growth of superconducting $\text{Bi}_2\text{Sr}_2\text{CaCu}_2\text{O}_{8+\delta}$ (Bi-2212) single crystal whiskers with a Te-doped method. We used a Te-doped precursor with the mixed pure powders Bi_2O_3 , SrCO_3 , CuO and TeO_2 . We have tried various stoichiometry of Ca and Cu with Te doping level and the best ratio was found to be $\text{Bi}_2\text{Sr}_2\text{Ca}_2\text{Cu}_{2.5}\text{Te}_{0.5}\text{O}_x$. Bi-2212 single crystal whiskers have grown through the pellet surface 2-4 mm in length and 20-100 μm in width. Characteristics of whiskers were investigated by the resistance-temperature (R - T), X-ray diffraction (XRD) and current-voltage (I - V) measurements.

The R - T characteristics in ab -plane of the whiskers showed that their $T_{c,on}$ and $T_{c,end}$ were about 106 K and 75 K, respectively and confirmed that the whiskers had Bi-2212 single crystal phase by XRD pattern. Above the transition temperature the whiskers shows metallic behaviour. The double phase transition in R - T characteristics indicated towards the existence of $\text{Bi}_2\text{Sr}_2\text{Ca}_2\text{Cu}_3\text{O}_{10+\delta}$ (Bi-2223). However with XRD the peak structure for Bi-2223 is less. The I - V curves showed multi-branch structures of intrinsic Josephson junctions (IJJs) as evidence of c -axis transport characteristics. These IJJs are arranged in series as an array.

REFERENCES

- [1] J. R. Gavaler, "Superconductivity in Nb/Ge films above 22 K" Appl. Phys. Lett. 23 480 (1973).
- [2] J.G. Bednorz and K. A. Muller, "Possible high T_c superconductivity in the Ba-La-Cu-O system" Z. Phys. B64,189 (1986).
- [3] M. K. Wu et al, "Superconductivity at 93 K in a new mixed-phase Y-Ba-Cu-O compound system at ambient pressure" Phys Rev Lett 58, 908 (1987).
- [4] S. Hikami et al, "High Transition Temperature Superconductor: Y-Ba-Cu Oxide" Jap. J. Appl. Phys. 26, L314, 1987.
- [5] H. Maeda, Y. Tanaka, M. Fukutomi and T. Asano, "A New High- T_c Oxide Superconductor without a Rare Earth Element", Jpn. J. Appl. Phys. 27 (1988), p. L209.
- [6] Z. Z. Sheng and A. M. Hermann, "Superconductivity in the rare-earth-free Tl-Ba-Cu-O system above liquid-nitrogen temperature", Nature 332 55 1988
- [7] Josephson B. D., "Possible new effects in superconductive tunnelling", Physics Letters 1 251 (1962)
- [8] Zimmerman J. E, Silver A.H., "Quantum effects in type II superconductors", Phys. Lett 10 47 (1964)
- [9] Anderson P. W., Dayem A. H., "Radio-Frequency Effects in Superconducting Thin Film Bridges", Phys. Rev. Lett. 13 195 (1964)
- [10] Clarke J., "Supercurrents in Lead-Copper-Lead Sandwiches", Proc. Roy. Soc. LondonA 308 447 (1969)

- [11] Clarke J., “Finite-Voltage Behavior of Lead-Copper-Lead Junctions”, Phys. Rev. B4 2963 (1971)
- [12] Arrington C. H., Deaver B. S., “Superconducting weak links formed by ion implantation”, Appl. Phys. Lett. 26 204 (1975)
- [13] Chaudari P., Mannhart J., Dimos D., Tsuei C. C., Chai J., Oprysko M. M., Scheuermann M., “Direct measurement of the superconducting properties of single grain boundaries in $\text{YBa}_2\text{Cu}_3\text{O}_{7+\delta}$ ”, Phys. Rev. Lett. 60 16 1653 (1988)
- [14] Kleiner R., Steinmeyer F., Kunkel G., Mueller, “Intrinsic Josephson effects in $\text{Bi}_2\text{Sr}_2\text{CaCu}_2\text{O}_8$ single crystals”, P. Phys. Rev. Lett. 68 2394 (1992)
- [15] Tinkham M 1996 “*Introduction to Superconductivity 2nd edn (New York: McGraw-Hill)*”
- [16] A. Barone and G. Paterno, “Physics and Applications of the Josephson Effects, John Wiley & Sons, New-York”, 1982.
- [17] Yu. I. Latyshev, J. E. Nevelskaya, and P. Monceau, “Dimensional Crossover for Intrinsic dc Josephson Effect in $\text{Bi}_2\text{Sr}_2\text{CaCu}_2\text{O}_8$ Bi-2212 Single Crystal Whiskers”, Phys. Rev. Lett. **77**, 932 (1996)
- [18] Yong-Joo Doh, Jinhee Kim and Kyu-Tae Kim, Hu-Jong Lee, “Microwave-induced constant voltage steps in surface junctions of $\text{Bi}_2\text{Sr}_2\text{CaCu}_2\text{O}_{8+\delta}$ single crystals”, Phys. Rev. B **61**, R3834 (2000)
- [19] H. B. Wang, P. H. Wu, T. Yamashita, “Terahertz Responses of Intrinsic Josephson Junctions in High T_c Superconductors”, Phys. Rev. Lett. **87**, 107002 (2001)
- [20] V. M. Krasnov, N. Mros, A. Yurgens, D. Winkler, “Fiske steps in intrinsic $\text{Bi}_2\text{Sr}_2\text{CaCu}_2\text{O}_{8+\delta}$ stacked Josephson junctions”, Phys. Rev. B **59**, 8463 (1999)
- [21] Kim S -J, and Yamashita T, “Fabrication and characteristics of submicron tunneling junctions on high T_c superconducting c -axis thin films and single crystals”, 2001 Jour. Appl. Phys. **89** 7675

- [22] V. P. Koshelets and S. Shitov, "Integrated superconducting receivers", *Supercond. Sci. Technol.* 13, R53 (2000).
- [23] R. Kleiner et al., "Intrinsic Josephson effects in $\text{Bi}_2\text{Sr}_2\text{CaCu}_2\text{O}_8$ single crystals", *Phys. Rev. Lett.* 68, 2394 (1992).
- [24] A. A. Yurgens, "Intrinsic Josephson junctions: recent developments", *Supercond. Sci. Technol.* 13, R85 (2000).
- [25] Y.-S. Lee, "Principles of Terahertz Science and Technology Springer", New York, 2009.
- [26] H. B. Wang et al., "Terahertz oscillation in submicron sized intrinsic Josephson junctions", *Appl. Phys. Lett.* 89, 252506 (2006).
- [27] M.-H. Bae, H.-J. Lee, J.-H. Choi, "Josephson-Vortex-Flow Terahertz Emission in Layered High- T_c Superconducting Single Crystals", *Phys. Rev. Lett.* 98, 027002 (2007).
- [28] K. Kadowaki et al., "Dynamical properties of Josephson vortices in mesoscopic intrinsic Josephson junctions in single crystalline $\text{Bi}_2\text{Sr}_2\text{CaCu}_2\text{O}_{8+\delta}$ ", *Physica C* 437-438, 111 (2006).
- [29] A. Irie, Y. Hirai, and G. Oya, "Fiske and flux-flow modes of the intrinsic Josephson junctions in $\text{Bi}_2\text{Sr}_2\text{CaCu}_2\text{O}_x$ mesas", *Appl. Phys. Lett.* 72, 2159 (1998).
- [30] V. M. Krasnov, N. Mros, A. Yurgens, and D. Winkler, "Fiske steps in intrinsic $\text{Bi}_2\text{Sr}_2\text{CaCu}_2\text{O}_{8+\delta}$ stacked Josephson junctions", *Phys. Rev. B* 59, 8463 (1999).
- [31] Bylander J, Duty T, and Delsing P "Current measurement by real-time counting of single electrons", 2005 *Nature* **434** **361**
- [32] Aassime A, Delsing P, and Claeson T, "A sensitive and fast radio frequency single-electron transistor", 2001, *Nanotechnology* **12** **96**.
- [33] S. M. Kim et al., "Fiske steps studied by flux-flow resistance oscillation in a narrow stack of $\text{Bi}_2\text{Sr}_2\text{CaCu}_2\text{O}_{8+\delta}$ junctions" *Phys. Rev. B* 72, 140504 (2005).

- [34] S. Madsen, G. Fillatrella, N. F. Pedersen, “Interaction between a BSCCO-type intrinsic Josephson junction and a microwave cavity”, *Eur. Phys. J. B* 40, 209 (2004).
- [35] L. Ozyuzer, A. E. Koshelev, C. Kurter, N. Gopalsami, Q. Li, M. Tachiki, K. Kadowaki, T. Yamamoto, H. Minami, H. Yamaguchi, T. Tachiki, K. E. Gray, W.-K. Kwok, and U. Welp, “Emission of Coherent THz Radiation from Superconductors”, *Science* 318, 1291 (2007).
- [36] H. B. Wang, S. Guenon, B. Gross, J. Yuan, Z. G. Jiang, Y. Y. Zhong, M. Grunzweig, A. Iishi, P. H. Wu, T. Hatano, D. Koelle, and R. Kleiner “Coherent Terahertz Emission of Intrinsic Josephson Junction Stacks in the Hot Spot Regime”, *Phys. Rev. Lett.* **105**, 057002 (2010)
- [37] S. Shamoto, S. Hosoya and M. Sato, “Single crystal growth of high- T_c superconductors”, *Solid State Commun.* 66 (1988), p. 195.
- [38] S. Takekawa, H. Nozaki, A. Umezono, K. Kosuda and M. Kobayashi, “Single crystal growth of the superconductor $\text{Bi}_{2.0}(\text{Bi}_{0.2}\text{Sr}_{1.8}\text{Ca}_{1.0})\text{Cu}_{2.0}\text{O}_8$ ”, *J. Cryst. Growth* 92 (1988), p. 687.
- [39] G. Balakrishnan, D. McK. Paul, M. R. Lees and A. T. Boothroyd, “Single crystal growth of $\text{Bi}_2\text{Sr}_2\text{CaCu}_2\text{O}_8$ using an infra-red image furnace”, *Physica C* 206 (1993), p. 148.
- [40] Yu. I. Latyshev, I. G. Gorlova, A. M. Nikitina, V. U. Antokhina, S. G. Zybtssev, N. P. Kukhta and V. N. Timofeev, “Growth and study of single-phase 2212 BSCCO whiskers of submicron cross-sectional area”, *Physica C* 216 (1993), p. 471.
- [41] I. Matsubara, R. Funahashi, T. Ogara, H. Yamashita, K. Tsuru and T. Kawai, “Growth mechanism of $\text{Bi}_2\text{Sr}_2\text{CaCu}_2\text{O}_x$ superconducting whiskers”, *J. Cryst. Growth* 141 (1994), p. 131.
- [42] R. K. Pandey, M. Hannan and K. K. Raina, “Single crystal growth of $\text{Bi}_2\text{CaSr}_2\text{Cu}_2\text{O}_{8+x}$ superconductor by travelling zone method”, *J. Cryst. Growth* 137 (1994), p. 268.

- [43] R. Kleiner, F. Steinmeyer, G. Kunkel and P. Müller, "Intrinsic Josephson effects in $\text{Bi}_2\text{Sr}_2\text{CaCu}_2\text{O}_8$ single crystals", *Phys. Rev. Lett.* **68** (1992), p. 2394.
- [44] M. Tachiki, T. Koyama and S. Takahashi, "Electromagnetic phenomena related to a low-frequency plasma in cuprate superconductors", *Phys. Rev. B* **50** (1994), p. 7065.
- [45] S.-J. Kim, Yu.I. Latyshev and T. Yamashita, "Submicron stacked-junction fabrication from $\text{Bi}_2\text{Sr}_2\text{CaCu}_2\text{O}_{8+\delta}$ whiskers by focused-ion-beam etching", *Appl. Phys. Lett.* **74** (1999), p. 1156.
- [46] Yu.I. Latyshev, M.B. Gaifullin, T. Yamashita, M. Machida and Y. Matsuda, "Shapiro Step Response in the Coherent Josephson Flux Flow State of $\text{Bi}_2\text{Sr}_2\text{CaCu}_2\text{O}_{8+\delta}$ ", *Phys. Rev. Lett.* **87** (2001), p. 247007.
- [47] M. Nagao, M. Sato, H. Maeda, S.-J. Kim and T. Yamashita, "Growth and superconducting properties of $\text{Bi}_2\text{Sr}_2\text{CaCu}_2\text{O}_{8+\delta}$ single-crystal whiskers using tellurium-doped precursors", *Appl. Phys. Lett.* **79** (2001), p. 2612.
- [48] L. R. Harriott, P. A. Polakos, and C. E. Rice, "High-resolution patterning of high T_c superconductors", *Appl. Phys. Lett.* **55**, 495 1989.
- [49] Q. Y. Ma, A. Wong, P. Dosanjh, J. F. Carolan, and W. N. Hardy, "A planar method for patterning of high-temperature superconducting films and multilayers", *Appl. Phys. Lett.* **65**, 240 1994.
- [50] F. X. Regi, J. Schneck, J. F. Palmier, and H. Savary, "70 K hysteretic Josephson effect in mesas patterned on $(\text{Bi,Pb})_2\text{Sr}_2\text{CaCu}_2\text{O}_y$ single crystals", *J. Appl. Phys.*, **76** 4426 1994.
- [51] Yu. I. Latyshev, J. E. Nevelskaya, "Critical currents across the layers of $\text{Bi}_2\text{Sr}_2\text{CaCu}_2\text{O}_x$ whiskers in a parallel magnetic field", *Physica C* **235-240** 2991 1994.
- [52] A. Yurgens, D. Winkler¹, T. Claeson¹, and N. V. Zavaritsky, "In situ controlled fabrication of stacks of high- T_c intrinsic Josephson junctions", *Appl. Phys. Lett.* **70**, 1760 1997.

- [53] L. N. Bulaevskii, J. R. Clem, L. I. Glazman, "Fraunhofer oscillations in a multilayer system with Josephson coupling of layers", *Phys. Rev. B* **46**, 350 (1992).
- [54] Kim S -J, Latyshev Yu I, and Yamashita T, "3D intrinsic Josephson junctions using *c*-axis thin films and single crystals", 1999 *Supercond. Sci. Technol.* **12** 729
- [55] Levin A A, Smolin I Y, Shepelev F Y "Causes of modulation and hole conductivity of the high- T_c superconductor $\text{Bi}_2\text{Sr}_2\text{CaCu}_2\text{O}_{8+\delta}$ according to X-ray single-crystal data", 1994 *J. Phys. Condens. Matter* **6**, 3539
- [56] T. Yamashita and M. Tachiki, "Single-Crystal Switching Gates Fabricated Using Cuprate Superconductors", *Jap. J. Appl. Phys. Part 1* 35 (1996) 4314.
- [57] R. M. Hazen, C. T. Prewitt, R. J. Angel, N. L. Ross, L. W. Finger, C. G. Hadjidakos, D. R. Veblen, P. J. Heaney, P. H. Hor, R. L. Meng, Y. Y. Sun, Y. Q. Wang, Y. Y. Xue, Z. J. Huang, L. Gao, J. Bechtold, and C. W. Chu, "Superconductivity in the high- T_c Bi-Ca-Sr-Cu-O system: Phase identification" *Phys. Rev. Lett.* 60, 1174 (1988).
- [58] Saini S, Kim G S, Kim S -J, "Characterization of Submicron Sized Josephson Junction Fabricated in a $\text{Bi}_2\text{Sr}_2\text{Ca}_2\text{Cu}_3\text{O}_{10+\delta}$ (Bi-2223) Single Crystal Whisker", 2010 *J. Supercond. Nov Magn* **23** 811
- [59] Latyshev Yu I, Kim S -J, and Yamashita T, "Experimental evidence for Coulomb charging effects in the submicron Bi-2212 stacks", 1999 *JETP Lett.* **69** 84
- [60] Warburton P A, Fenton J C, Korsah M, and Grovenor C R M, "Josephson current suppression in three-dimensional focused-ion-beam fabricated sub-micron intrinsic junctions", 2006 *Supercond. Sci. Technol.* **19** S187
- [61] Y.F. Yan, P. Matl, J. M. Harris, and N.P. Ong, "Negative magnetoresistance in the *c*-axis resistivity of $\text{Bi}_2\text{Sr}_2\text{CaCu}_2\text{O}_{8+\delta}$ and $\text{YBa}_2\text{Cu}_3\text{O}_{6+\delta}$ ", *Phys. Rev. B*, vol. 52, 1995, pp. R751-R754.
- [62] L.B. Ioffe, A.I. Larkin, A.A. Varlamov, L. Yu "Effect of superconducting fluctuations on the transverse resistance of high- T_c superconductors", *Phys. Rev. B*, vol. 47, 1993, pp. 8936-8941. *Lett.* 74, 1156 (1996).

- [63] H. Nobumasa, K. Shimizu, Y. Kitano and T. Kawai, "High T_c Phase of Bi-Sr-Ca-Cu-O Superconductor", Jpn.J. Appl. Phys. 27, L846 (1988).
- [64] T. Hatano, K. Aota, S. Ikeda, K. Nakamura and K. Ogawa, "Growth of the 2223 Phase in Lead Bi-Sr-Ca-Cu-O System", J. Appl. Phys. 27, L2055 (1988).
- [65] Q. Feng, H. Zhang, S. Feng, X. Zhu, K. Wu, Z. Liu and L. Xue, "The process of forming 2223 phase from 2212 phase in Bi(Pb)-Sr-Ca-Cu-O System", Solid State Communication. 78, 609 (1991).
- [66] U. Endo, S. Koyama and T. Kawai, "Preparation of the High- T_c Phase of Bi-Sr-Ca-Cu-O Superconductor", Jpn. J. Appl. Phys. 27, L1476 (1988).
- [67] I. Matsubara, R. Funahashi, T. Ogura, H. Yamashita, Y. Uzawa, K. Tanizoe and T. Kawai, "Conversion of $\text{Bi}_2\text{Sr}_2\text{CaCu}_2\text{O}_x$ whiskers to the $\text{Bi}_2\text{Sr}_2\text{Ca}_2\text{Cu}_3\text{O}_x$ phase by annealing in powder", Physica C 218, 181 (1993).